





Nuclear Science User Facilities 995 MK Simpson Blvd. Idaho Falls, ID 83401-3553 nsuf.inl.gov

On the front and back cover: University of Michigan's dual ion beam interface with the FEI 300 kV TF30 transmission electron microscope for in situ ion irradiation (credit: University of Michigan).

#### Disclaimer

This information was prepared as an account of work sponsored by an agency of the U.S. Government. Neither the U.S. Government nor any agency thereof, nor any of their employees, makes any warranty, expressed or implied, or assumes any legal liability or responsibility for the accuracy, completeness, or usefulness, of any information, apparatus, product, or process disclosed, or represents that its use would not infringe privately owned rights. References herein to any specific commercial product, process, or service by trade name, trade mark, manufacturer, or otherwise, does not necessarily constitute or imply its endorsement, recommendation, or favoring by the U.S. Government or any agency thereof. The views and opinions of authors expressed herein do not necessarily state or reflect those of the U.S. Government or any agency thereof.

Editors: Tiera Cate, Heather Rohrbaugh, Rebecca Jones, Jeffrey Pinkham

Writers: Tiera Cate and Jeannette Boner

Graphic Designers: Barry Pike III, Kristyn St. Clair, Lauren Perttula

## CONTENTS

Nuclear Science User Facilities	
Our NSUF Program Office Team	6
From the NSUF Director	8
■ NSUF Overview	
NSUF By The Numbers	12
NSUF Across The Nation	12
• From The Year	16
Capability Updates	
Facilities and Capabilities	22
NSUF Features	
Material Additions to the NMFL	24
Researcher Highlights	28
Activated Materials Laboratory	2 /

# CONTENTS

NSUF Awarded Projects	
Awarded Projects	36
• In Situ Ion Irradiation to add Irradiation Assisted Grain Growth	
to the Marmot Tool	44
• Ion Irradiation for High Fidelity Simulation of High Dose Neutron Irradiation	58
<ul> <li>Bubble Formation of In Situ He-Implanted 14YWT and CNA</li> </ul>	
Advanced Nanostructured Ferritic Alloys	62
Changes in Mechanical and Chemical-Structural Properties	
of Gamma Irradiated Calcium Silicate Hydrates to an Absorbed Dose of 200 MGy	
with Respect to Pristine Samples	66
In Situ SEM Irradiation Enhanced Creep Studies of 14 YWT	70
• Ion Irradiation of ThO $_2$ and UO $_2$ Single Crystals	72
<ul> <li>Defect Clustering in 316H Stainless Steel and High Entropy Alloy</li> </ul>	
Under <i>In-situ</i> Irradiation at 600-700°C	76
<ul> <li>Atom Probe Characterization of Neutron Irradiated Commercial</li> </ul>	
ZIRLO® and AXIOM X2® Alloys	80
Resources	
NSUF List of Acronyms	84
NCLIE Inday	06



### OUR NSUF PROGRAM OFFICE **TEAM**



J. Rory Kennedy, Ph.D. Director (208) 526-5522 rory.kennedy@inl.gov

Dan Ogden Deputy Director (208) 526-4400 dan.ogden@inl.gov



Simon Pimblott, D. Phil. Chief Post Irradiation Scientist (208) 526-7499 simon.pimblott@inl.gov



Keith Jewell, Ph.D. Technical Lead (208) 526-3944 james.jewell@inl.gov



**Travis Howell** Experiment Manager (208) 526-3817 travis.howell@inl.gov



William McClung Project Scheduler william.mcclung@inl.gov



Chief Irradiation Scientist (208) 533-8210 brenden.heidrich@inl.gov

Brenden Heidrich, Ph.D.



**Collin Knight** Post Irradiation Examination Project Manager (208) 533-7707 collin.knight@inl.gov



**Katie Anderson** Experiment Manager (208) 526-0049 katie.anderson@inl.gov

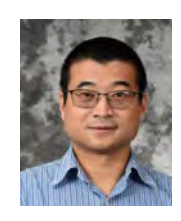


**Matthew Arrowood** Experiment Manager (208) 526-3527 matthew.arrowood@inl.gov



Colin Judge, Ph.D. Industry Program Lead (Outgoing April 2021) (208) 526-4514 colin.judge@inl.gov





Peng Xu, Ph.D. Industry Program Lead (Incoming April 2021) (208) 533-8163 peng.xu@inl.gov

Lindy Bean Consolidated Innovative Nuclear Research Administrator (208) 526-4662 lindy.bean@inl.gov



Je Rad Ex, (20 jet

Jeff Benson Rapid Turnaround Experiment Administrator (208) 526-3841 jeff.benson@inl.gov

Kelly Cunningham Nuclear Fuels and Materials Library Coordinator and RTE Administrator (208) 526-2369 kelly.cunningham@inl.gov





**Tiera Cate**Communications Liaison
(208) 526-4828
tiera.cate@inl.gov

Rachel Jones Planning and Financial Controls Specialist (208) 526-4315 rachel.jones@inl.gov





**Renae Tripp** Administrative Assistant (208) 526-6918 renae.soelberg@inl.gov

**Dain White** Technical Lead Software Engineer (208) 533-8210 dain.white@inl.gov



### DIRECTOR

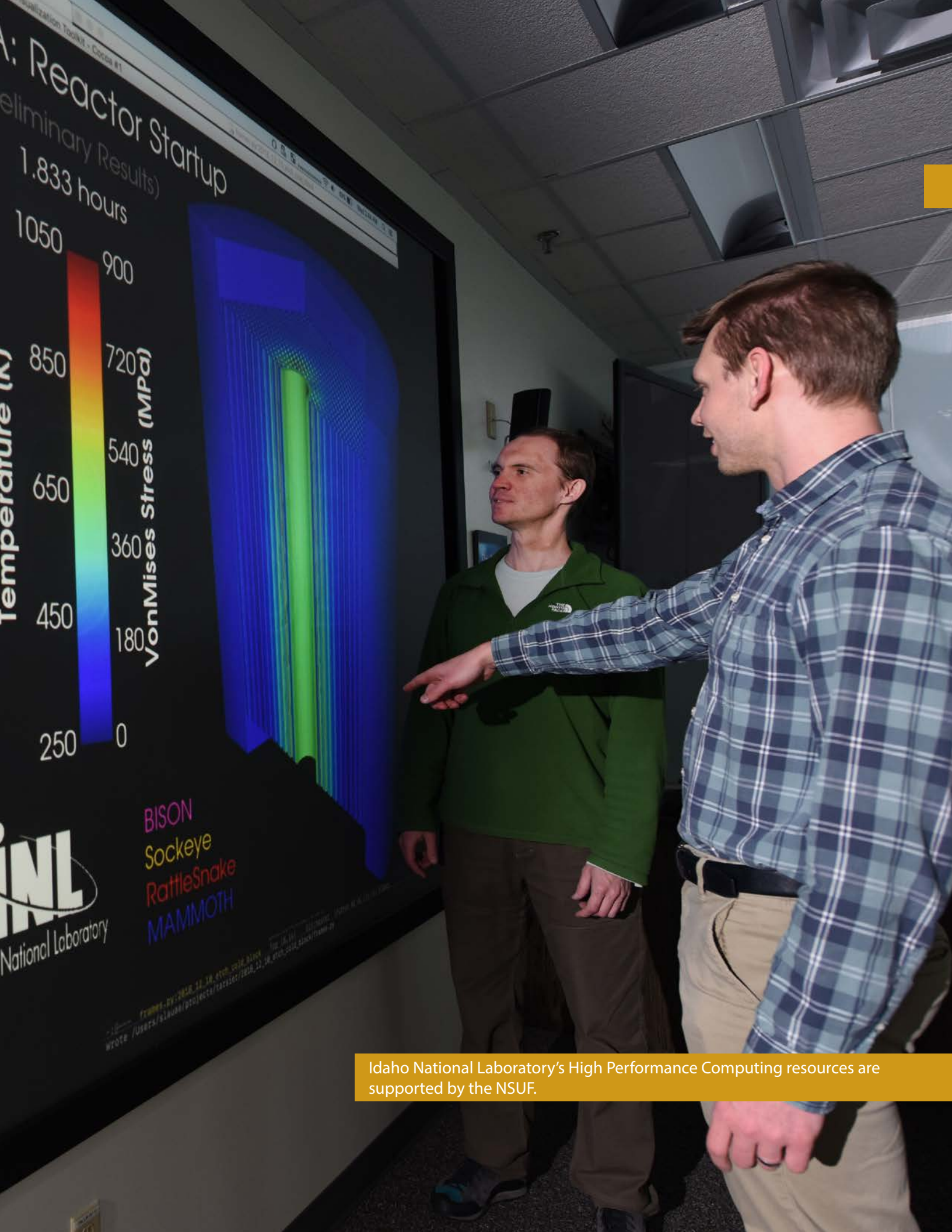


J. Rory Kennedy, Ph.D. Director (208) 526-5522 rory.kennedy@inl.gov

he Nuclear Science User Facilities (NSUF) had high hopes for 2021 compared to 2020 when we were hit by the COVID-19 pandemic, a significant effective budget shortfall, and other regrettable events. Unfortunately, both the COVID-19 pandemic and the significant reduction in funds experienced in fiscal year (FY) 2020 continued into FY 2021 (reduction of ~\$20 million or 2/3 of our effective budget compared to 2019). This caused even greater challenges, such has allowing for only one Rapid **Turnaround Experiment** (RTE) solicitation and halting most update efforts to our databases. Despite all of that, the NSUF staff, facility partners, and our engaged users enabled the NSUF to still have a successful year. The quality

of the proposals submitted continued to be exceptional and we were able to make 34 total awards including 29 RTEs and five Consolidated Innovative Nuclear Research (CINR) projects, with the latter amounting to about \$4M in support, the same as we were able to do in FY 2020.

As begun in 2020, staff members in the NSUF Program Office continued working from home in 2021. We were able to maintain communication and productivity with our users and our partner facilities, although some NSUF partner facilities continued to experience some level of restricted or reduced operations. The NSUF worked to remain flexible, addressing issues as they arose and finding the best solution for the circumstances. Contributing





to this was Tiera Cate, who we welcomed as our new communications lead, and Peng Xu, who joined the NSUF as our new industry lead. I want to thank our past communications lead, Tiffany Adams for her excellent work, and Colin Judge for his outstanding job as our prior industry lead and wish them all the best in their new adventures. We also added two new members to our NE-5 oversight at DOE-HQ: Suibel Schuppner as Director of the **Nuclear Energy Technologies** Office and Melissa Bates as the **Enabling Technologies Team** Leader under Suibel.

Although we faced some serious challenges in FY 2021, please don't get the impression that it was all doom and gloom. We brought a record thirteen CINR projects to conclusion; completed 43 of 56 RTEs, finished off fourteen neutron irradiations in five reactors; added over 950 samples to the Nuclear Fuels and Materials Library (NFML) while linking the NFML search function to the NSUF projects database; and began the application of the Fuels and Materials Understanding Scale (FaMUS) methodology to NSUF historical data to

begin a quantitative analysis of the NSUF's impact. And I'm sure the improvements to our website and search capabilities have been helpful to all.

The productivity from NSUF users continued to grow in FY 2021, producing a record 175 peer reviewed publications in the fiscal year. As of the time of this writing, NSUF supported authors have published a total to 607 peer reviewed journal publications, which have been cited 5,794 times, resulting in a cumulative h-index of 35 (Clarivate Web of Science). As noted in previous

years, the *Journal of Nuclear Materials* continues to be the preferred venue for NSUF research publications. I want to acknowledge our users who presented virtually at the three NSUF sessions at the American Nuclear Society (ANS) 2020 Winter Meeting and two sessions at the ANS 2021 Annual Meeting. The talks were excellent and I look forward to organizing and chairing more sessions in FY 2022, so please prepare your abstracts early as you will be hearing from me.

On the international front, we continued our leadership, together with the United Kingdom's National Nuclear User Facility (NNUF), of the US-UK Nuclear Energy R&D Cooperative Action Plan's **Enabling Technology Working** Group and also moved forward on our important collaboration with the Belgian Nuclear Research Centre in executing the DISECT project (Disc Irradiation for Separate Effects testing with Control of Temperature) designed to better understand metallic fuel behavior.

Finally, calendar year 2022 will be my last year leading the NSUF as Director. Since there will be a new director at the

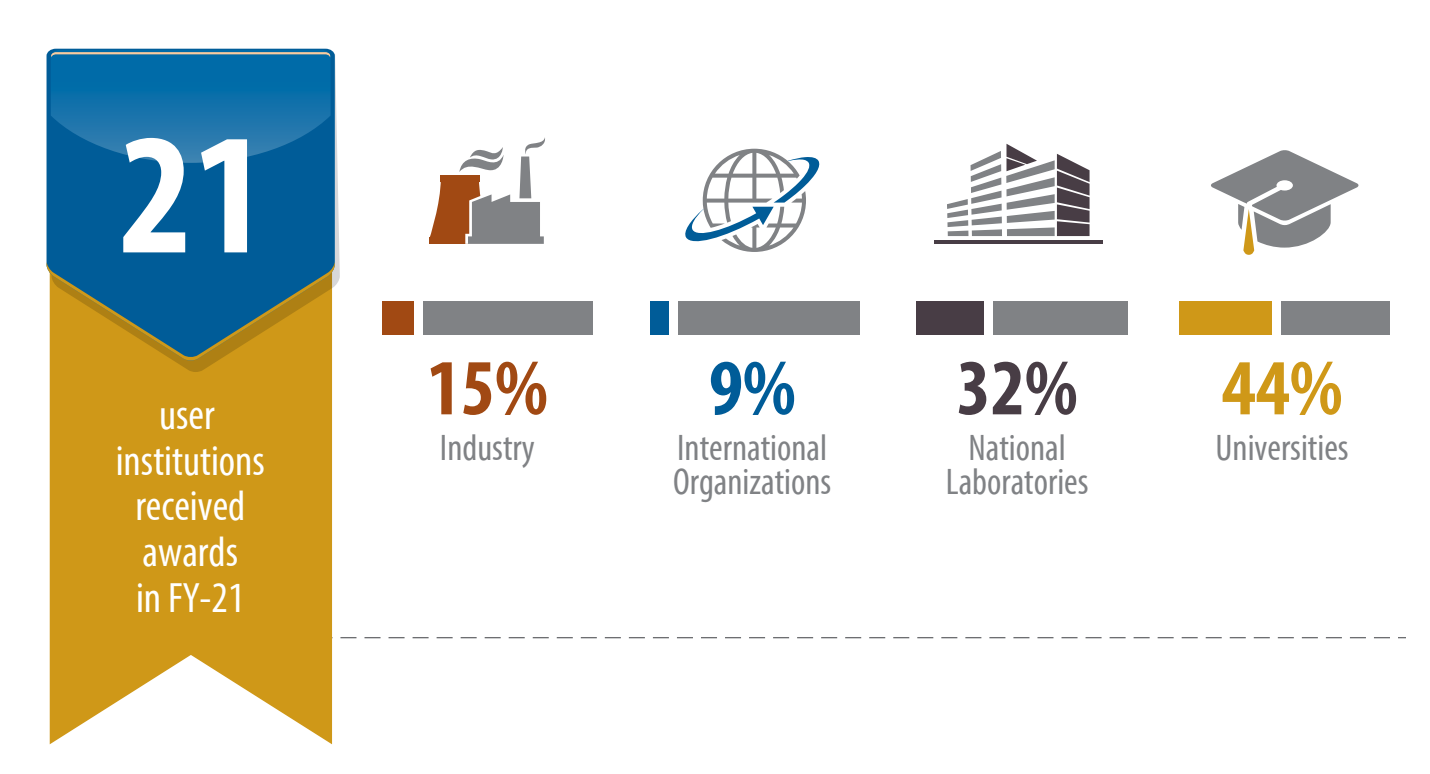
time of writing the FY 2022 Annual Report, this may be my last "From the NSUF Director" contribution. As such, I would like to thank everyone I have had the pleasure of working and interacting with over the nine years of my tenure, including all the NSUF staff members, all the staff and instrument scientists at INL and the partner facilities, members of the Science Review Board, the Users Organization, the DOE Office of Nuclear Energy staff for their unrelenting support, and, of course, our users. It has been an exceptional experience and I believe we have made remarkable contributions to the science and engineering needed to advance nuclear energy. I will continue to work throughout 2022 to see our budget restored so that the NSUF can continue to conduct its cutting edge, innovative research going into the future.

Rory

J. Rory Kennedy, Ph.D.

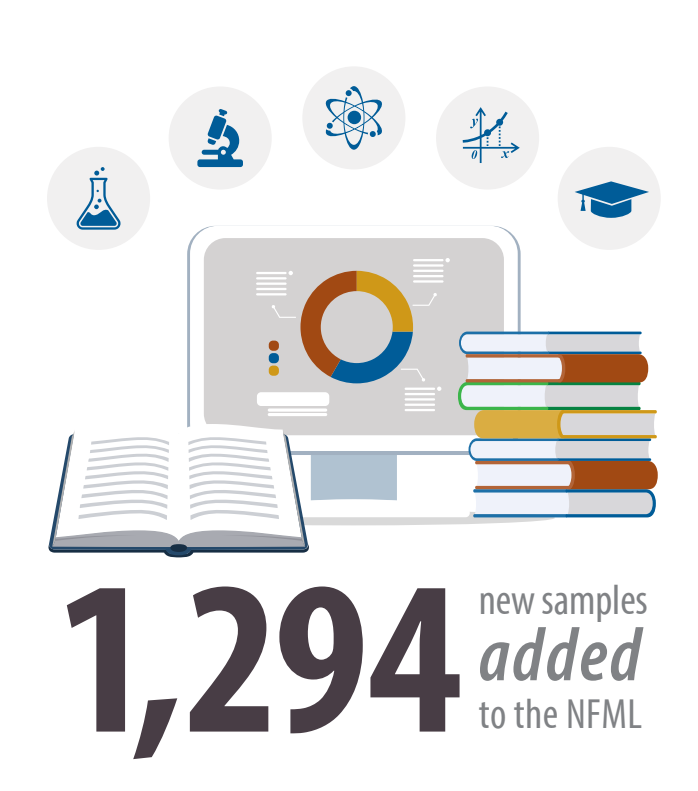
## NSUF BY THE NUMBERS

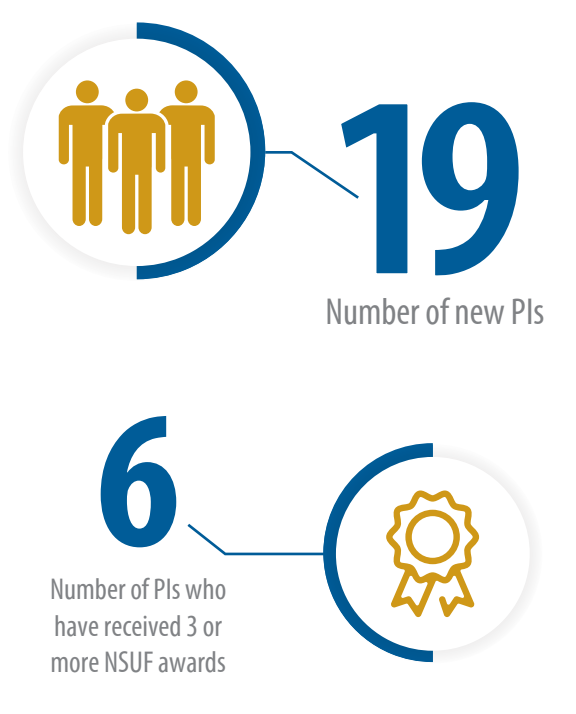




## 31) PERCENT

of projects involve a graduate student, either as a PI or a collaborator





### NSUF ACROSS THE NATION



#### **NSUF Partner Institutions**



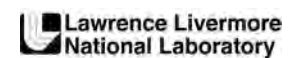














































#### **NSUF User Institutions (FY-21)**

Florida

University of Florida

Idaho

Idaho National Laboratory

Illinois

University of Illinois

Massachusetts

Massachusetts Institute of

**Technology** 

Michigan

University of Michigan

**New York** 

General Electric Global

Research

**North Carolina** 

**Electric Power Research** 

Institute

North Carolina State University

Oregon

Oregon State University

Pennsylvania

Carnegie Mellon University

Tennessee

Oak Ridge National Laboratory

University of Tennessee

**Texas** 

Southwest Research Institute

Texas A&M University

University of North Texas

Utah

**Brigham Young University** 

Washington

Pacific Northwest National

Laboratory

Wisconsin

University of Wisconsin

Italy

Italian Institute of Technology

Japan

Nagoya University

**United Kingdom**University of Oxford

### THE YEAR

The NSUF has seen great success this year and has many exciting things to highlight. In FY-21, examples of this success included the NSUF completing all 10 Level 2 milestones on or ahead of schedule, logging a record number of publications, adding over 1,294 samples to the Nuclear Fuels and Materials Library (NFML), organizing several NSUF sessions at conferences, and much more. In the following paragraphs, some of these critical achievements are highlighted in greater detail.

### **MARMOT Validation Project**

The NSUF began irradiation of the MARMOT Validation Project (MVP) in the Advanced Test Reactor (ATR). This experiment will provide unique data on U-Zr fuel and will allow the validation of microstructural evolution models in MARMOT, giving a direct correlation of changes in physical properties with specific irradiation-induced

microstructural features.

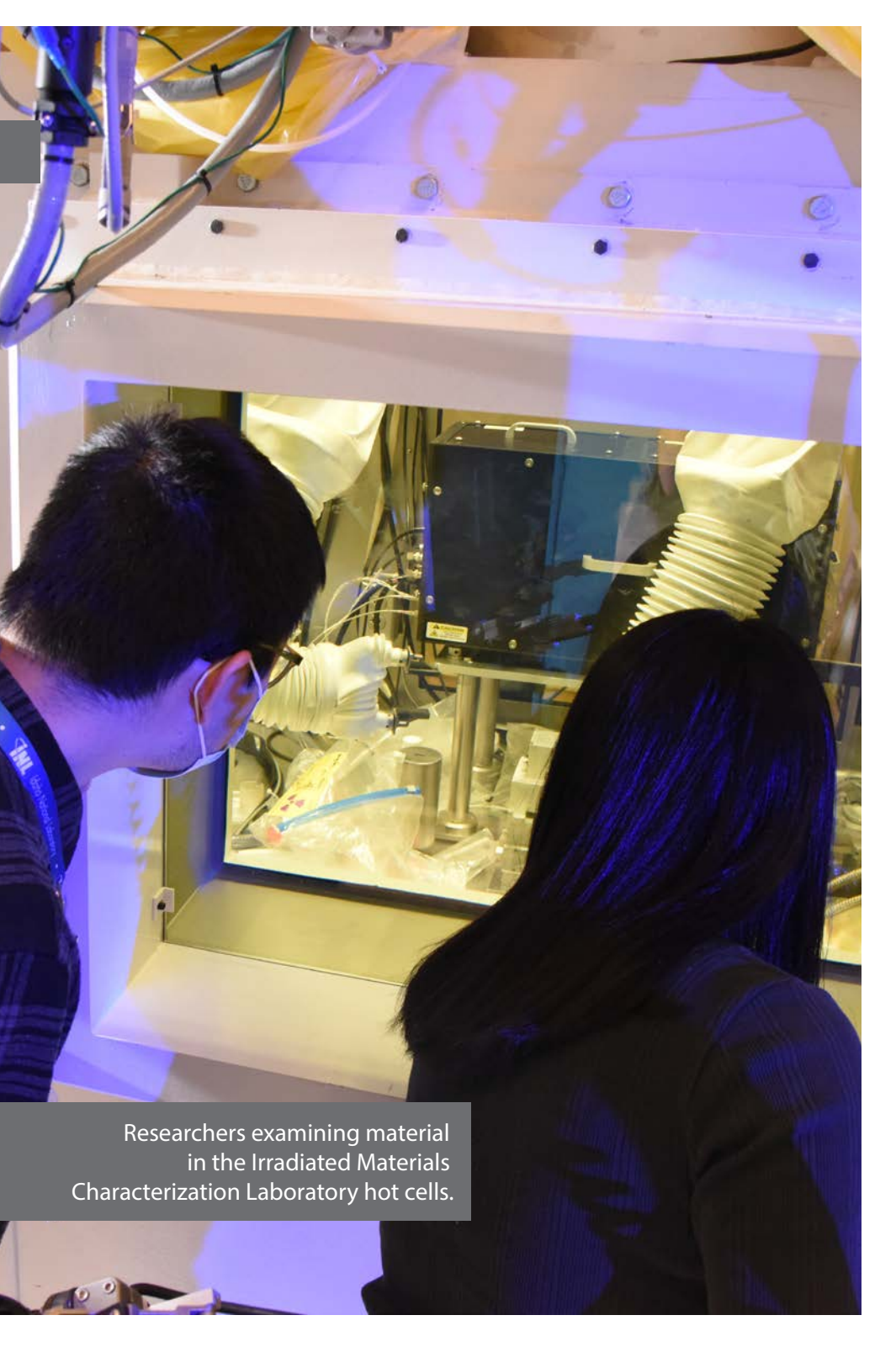
This experiment provides first of a kind information for direct validation of MARMOT by conducting detailed two- and three-dimensional characterization of the dimensions, microstructure and thermal properties of the same specimens and sister

specimens of U-Zr fuels prior to and after irradiation. The availability of accurate fuel (and material) models at this scale is key to decreasing the time required for nuclear fuel and material development and licensing.

Preirradiation characterization of the specimens has been performed at the National Synchrotron Light Source II (NSLS-II), an NSUF partner facility, to provide detailed lattice and microstructure information. The first capsule of samples has completed irradiation in ATR, with the three remaining capsules to be removed after the next 60day ATR cycle. This irradiation schedule supplies a wide range of fission burnup for the fueled specimens.







#### **SAM-2 Experiment**

The NSUF SAM-2 (Sample-2) irradiation experiment completed fabrication and inspection and is currently undergoing irradiation in ATR. The experiment will add materials to the NFML. The materials will be used for studies to understand the complex relationship between the electronic structure and the thermal and mechanical properties of high-purity neutron transmutation doped SiC.

The full project will span the range of SiC doping resistivity from the onset of semiconducting behavior to near metallic resistivity levels and will evaluate the competitive factors of transmutation doping compared to increased resistivity caused by lattice damage from fast neutron collisions. Post irradiation examination (PIE) will be performed over a range of temperatures to study the effects of the lattice damage.

The first three capsules of the SAM-2 project have completed irradiation in ATR and have been shipped to the Hot Fuels Examination Facility (HFEF) hot cell for disassembly.

#### **NSUF sessions at ANS**

**NSUF Director Rory Kennedy** organized and chaired three sessions at the American Nuclear Society (ANS) 2020 Winter Meeting and two NSUF sessions at the ANS 2021 Annual Meeting to update attendees on the organization's contributions to advanced nuclear research. These biyearly forums, as well as several other meetings, gather individuals from across national laboratories, academia, and industry to discuss advancements in nuclear energy.

The NSUF's sessions provide a platform for its users to share their research with colleagues across the nuclear energy sector. Due to travel restrictions from the COVID-19 pandemic, the sessions were held virtually which allowed more people to hear about the work that the NSUF helps bring to life.

Forums, such as the ANS meetings, allow researchers to share their groundbreaking research with a broad audience. They also serve as an avenue for collaboration, networking, and growth. The ability to highlight the impactful work that the organization makes possible is critical to the NSUF's continued success.



The Advanced Test Reactor at Idaho National Laboratory.

#### **NSERT Project**

The NSUF completed irradiation in ATR of the Nanostructured Steels for Enhanced Radiation Tolerance (NSERT) project that tested nanostructured austenitic and ferritic/martensitic steels. These steels were produced by two innovative, low cost manufacturing techniques for enhanced irradiation tolerance under light water reactor conditions.

In this project, specimens produced by two distinct methods, equal channel angular pressing and high pressure torsion, yield a fine and nanograined microstructure are being compared against the

standard cast coarse grained microstructure for irradiation tolerance. Samples were irradiated at two temperatures (300°C and 500°C) to two damage levels (2 dpa and 6 dpa). The 2 dpa specimens have been disassembled in the HFEF hot cell and are currently undergoing tensile testing and microscopy. The 6 dpa specimens are awaiting disassembly and will be scheduled for PIE.

### UPDATES

#### New Transmission Electron Microscope installed, advances nuclear innovation

A new transmission electron microscope (TEM) will be part of the Microscopy and Characterization Suite (MaCS), a **Nuclear Science User Facilities** laboratory accessible to students, faculty and other researchers at the Center for **Advanced Energy Studies** (CAES) universities. The new TEM will help with the analysis and development of advanced materials critical to the nation's new energy landscape. The TEM is more technologically advanced than the current TEM resources at CAES in several aspects.

The new TEM provides a broader electron energy range (30kV-300kV) for characterization, enabling research on a wider range of materials, from those that are sensitive to high energy electron beams to high atomic number materials, such as uranium.

It offers an energy resolution of better than 0.2 eV. This improvement enables the study of stoichiometry changes in oxide fuels, chemistry of fission products in nuclear fuels, and oxidation/corrosion behavior of metals and ceramics.

The TEM is equipped with a next generation Cs probe corrector S-CORR, which provides improved spatial resolution at low accelerating voltages, enabling analysis of light elements. It also has an electron microscope pixel array detector (EMPAD), which can obtain more than 1,000 diffraction patterns per second, which can capture dynamic material behavior such as phase changes and crystallization in harsh environments.

Finally, the TEM is equipped with a double corrector (probe and image) configuration making

it capable of achieving pointresolution close in value to the information limit of the system.

The TEM is designed to create opportunities for collaborative materials research. CAES is also equipped with complementary materials analysis instrumentation (including a focused ion beam and local electron atom probe) that will enable complete sample preparation and analysis in one location.

These complementary technologies will advance the timeline for nuclear innovation, accelerate modeling efforts needed for the discovery and qualification of materials for nuclear applications, and allow investigation of defects in functional energy materials found in batteries with atomic precision.

The TEM will provide a new perspective on the dynamic effects of irradiation damage, diffusion mechanisms and kinetics, as well as plasticity, which must be understood to advance materials in the extreme environments such seen in a reactor core. Furthermore, it will enable state-of-the-art atomic scale chemical imaging, paired with 3D tomography capability, facilitating new understanding of reacting interfaces of materials, providing immediate advances to collaborative research underway.

The NSUF is thrilled to bring these exciting new capabilities to its users and advance collaborative research, education, and innovation!



# FACILITIES AND CAPABILITIES

Partner Institution	Facilities					
Argonne National Laboratory	Intermediate Voltage Electron Microscopy (IVEM) Tandem Facility		<b>√</b>		<b>√</b>	
Brookhaven National Laboratory	National Synchrotron Light Source II					<b>√</b>
Center for Advanced Energy Studies	Microscopy and Characterization Suite (MaCS)		<b>√</b>			
Lawrence Livermore National Laboratory	Center for Accelerator Mass Spectrometry				<b>√</b>	
Los Alamos National Laboratory	Lost Alamos Neutron Scattering Center - Lujan Center Beamlines, Plutonium Surface Science Laboratory					<b>√</b>
Massachusetts Institute of Technology	Massachusetts Institute of Technology Nuclear Reactor, Massachusetts Institute of Technology Reactor	<b>✓</b>	<b>√</b>			
North Carolina State University	PULSTAR Reactor	<b>√</b>				<b>√</b>
Oak Ridge National Laboratory	High-Flux Isotope Reactor, Irradiated Fuels Examination Laboratory, Irradiated Materials Examination and Testing Facility, Low Activation Materials Design and Analysis Laboratory	<b>√</b>	<b>√</b>	<b>√</b>		
The Ohio State University	The Ohio State University Research Reactor	<b>√</b>		<b>√</b>		
Pacific Northwest National Laboratory	Materials Science and Technology Laboratory, Radiochemical Processing Laboratory		<b>√</b>			

- ✓ Neutron Irradiation
- ✓ Post Irradiation Examination (PIE)
- ✓ Gamma Irradiation
- ✓ Ion Beam Irradiation
- ✓ Characterization Beamline (Neutron, Positron, or X-ray)

Partner Institution	Facilities					
Purdue University	Interaction of Materials with Particles and Components		<b>√</b>		<b>✓</b>	
Sandia National Laboratories	Annular Core Research Reactor, SNL Ion Beam Laboratory, Sandia Pulse Reactor Facility Critical Experiment, Gamma Irradiation Facility	<b>√</b>	<b>√</b>	<b>√</b>		
Belgian Center for Nuclear Research (SCK/CEN)	Belgian Reactor 2, Laboratory for High and Medium Activity	<b>✓</b>	<b>√</b>			
Texas A&M University	Accelerator Laboratory				<b>✓</b>	
University of California, Berkely	Nuclear Materials Laboratory		<b>√</b>			
University of Florida	Nuclear Fuels and Materials Characterization		<b>√</b>			
University of Michigan	Irradiated Materials Testing Laboratory, Michigan Ion Beam Laboratory, Michigan Center for Materials Characterization		<b>✓</b>		<b>✓</b>	
University of Wisconsin	Characterization Laboratory for Irradiated Materials, University of Wisconsin Ion Beam		<b>√</b>		<b>✓</b>	
Westinghouse	Churchill Laboratory Services		<b>/</b>			

### TO THE NMFL

#### Not your typical library: Expanding the NFML for nuclear research

By Tiera Cate, INL Communications and Outreach

The Nuclear Fuels and Materials Library (NFML), owned by the U.S. Department of Energy's Office of Nuclear Energy and curated by the Nuclear Science User Facilities (NSUF), is the largest global open archive of high value irradiated fuel and material samples.

The NFML includes samples from real world components retrieved from decommissioned power reactors, along with donations from other sources. With the addition of unique, relevant samples to its inventory and a larger presence within the national and international nuclear community, the NFML's value continued to increase in FY 2021.

The NSUF expects the library to continue to grow. "In addition to adding samples from NSUF-

awarded projects, we are working on getting harvested material from the San Onofre Nuclear Generating Station that is being dismantled," said Kelly Cunningham, the NFML coordinator. Opportunities to harvest samples from domestic and international test reactors moved forward through contracts and collaborations with other national laboratories and industry.

Any new additions offer opportunities for future nuclear researchers to continue the advancement of the nuclear mission. Material assets added to the NFML are safeguarded from being disposed of as waste or lost to long-term storage.

The NFML works to ensure it remains inclusive and accessible. "A major improvement was the implementation of a new portal interface," said Dain White, the technical lead software engineer for NSUF. "Previously, the library was only viewable within the context of all projects, and the user had to differentiate between projects with samples available for additional research and all other projects."

To fix this, "project data was filtered to find projects with available samples, which were then integrated into a system that shows available samples by material," said White. "Within this interface, users can switch views to see samples by project or material. The system can also search available samples by a range of irradiation conditions such as dose, temperature, or fluence."

The NFML initiative maximizes the value of previous and ongoing nuclear materials and fuels irradiation test campaigns. In FY 2021, much progress was made toward

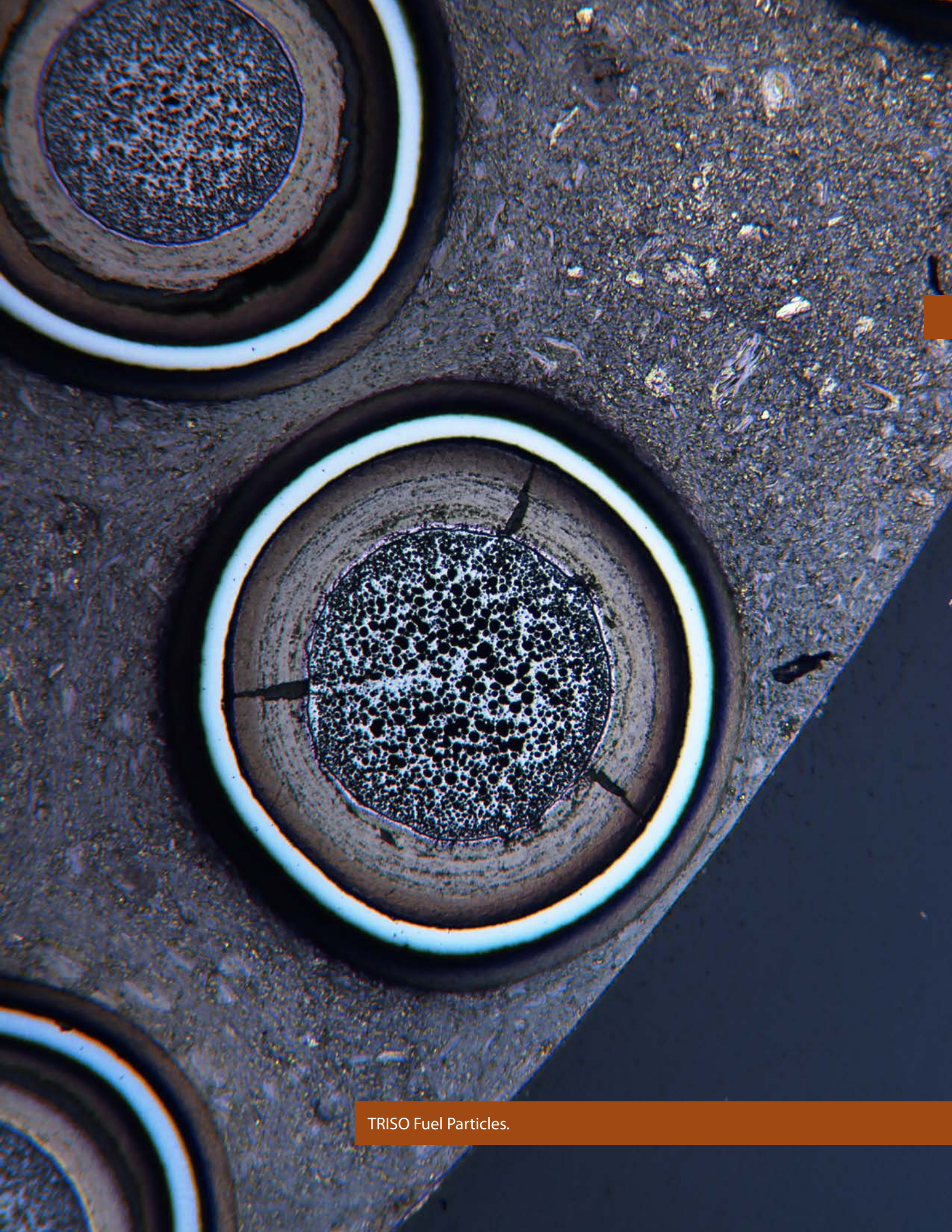




Figure 1. (Left) Unirradiated disks from a University of Central Florida project.

Figure 2. (Right) Tristructural isotropic (TRISO) particle sample.

adding historic material that must be maintained and kept available for nuclear research. Samples from a long-canceled DOE program were added, and many more from international projects and commercial reactors are in the process of being transferred.

As the curator of these valuable unused or residual fuels and materials, the NSUF maintains the physical inventory and material provenance, and ensures that the samples and associated information remain available to researchers. The library sees NSUF users consistently utilizing the samples, with an average of about 12% of Rapid Turnaround Experiment proposals requesting NFML samples.

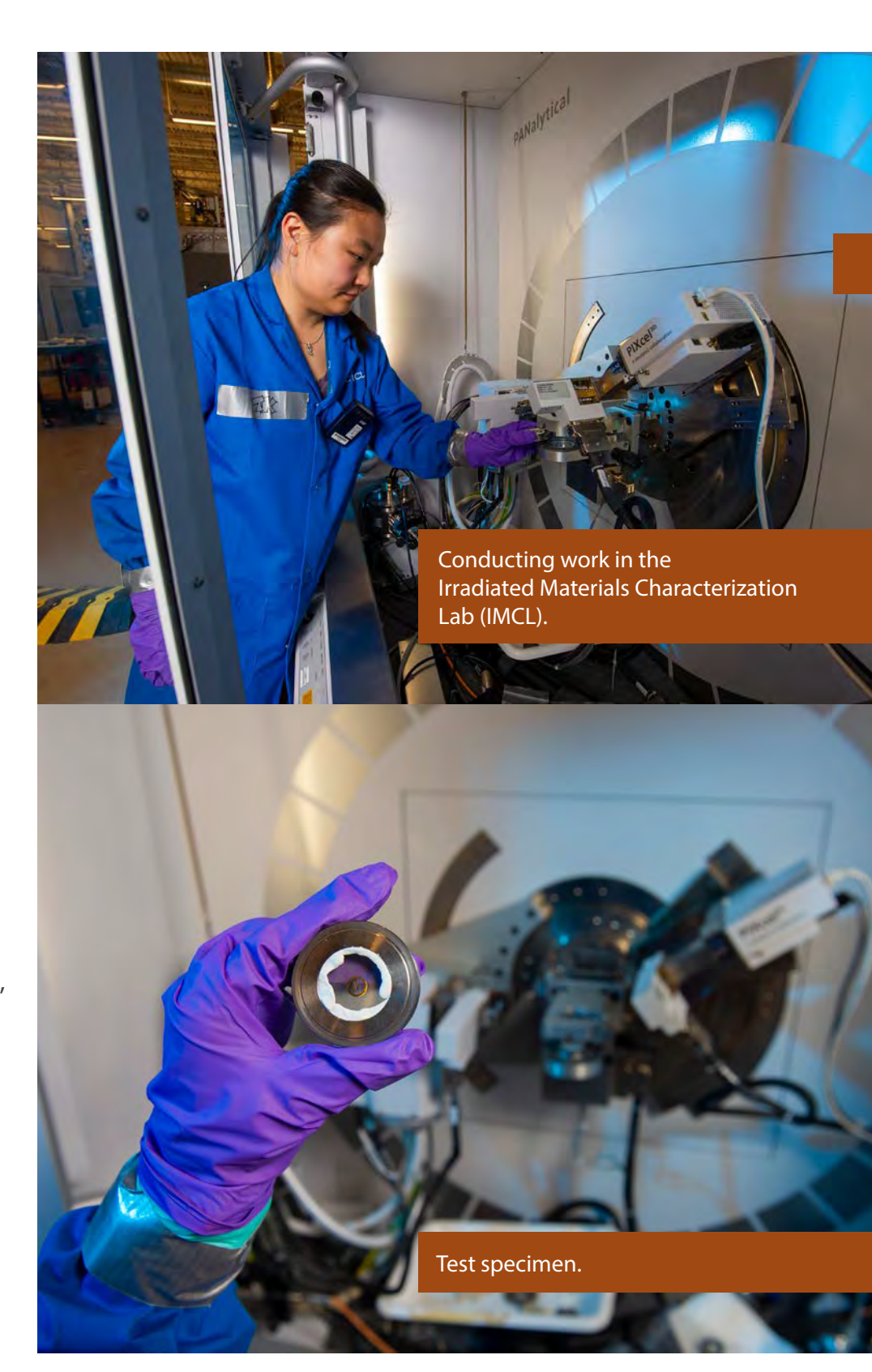
Thousands of specimens that had been irradiated as part of NSUF competitively awarded research projects have been added to the NFML, bringing the total to more than 8,000 samples in the library. Everything in the NFML is available to the nuclear research community, either through a peer-reviewed proposal process or by direct programmatic request.

As with any great endeavor, it doesn't come without hurdles. "Title transfers from donated samples can be challenging," said Cunningham. "Many samples must include an official transfer. A DOE transfer must be authorized by the originating program manager. A third party transfer must be

done via legal Transfer of Title and Ownership document. Individuals that donate samples may have possession of samples from completed projects where the original owner is difficult to find."

Both domestically and internationally, the NFML is recognized as an archive that will responsibly curate crucial (and irreplaceable) fuels and materials needed for research that can help propel nuclear power toward being an accepted, safe, cost effective, sustainable energy solution.

"The NFML provides researchers access to thousands of unique nuclear material and samples along with accompanying provenance, related publications and collaboration contacts," said Cunningham. "Coupled with NSUF's resources, the NFML will continue to be crucial to our knowledge of irradiation effects on materials, which will lead to longer lasting, safer, and more cost effective nuclear energy reactors."



### HIGHLIGHTS



#### **Assel Aitkaliyeva**

By Jeannette Boner

Assel Aitkaliyeva studies nuclear fuels as an assistant professor in the Department of Materials Science and Engineering at the University of Florida. While her specific area of study is critical to understanding nuclear fuels, she laughs and adds, "And I've always liked destroying things."

This is a funny comment for someone who looks at the research that is required to better understand performance of nuclear fuels, but Aitkaliyeva is breaking apart the science to reach new conclusions.

"If you are looking at fuels, the goal is to extend life," she said. "Light water reactor fuels are discharged at lower burnups because we don't have enough data about how these fuels perform at high burnups. We could potentially push these fuels to higher burnup."

Understanding the full life cycle of fuels is also critical to new and developing reactor design and technology.

"It's two-fold," Aitkaliyeva said.
"On the nuclear side, we are very application driven, but there are a lot of scientific questions. And there is still a lot of science there that hasn't been touched. Materials scientists like me get to be the first to look at the complicated behavior of the fuels and answer outstanding questions."

Aitkaliyeva earned her undergraduate degree at Kazakh State University in nuclear physics and went on to study nuclear engineering at Texas A&M University, completing a master's and doctorate. "While working on my master's degree, I discovered that I was passionate about the materials science aspect of the nuclear industry," she recently told the Journal of Materials. "My earlier exposure

to physics and engineering provided me with a unique perspective, and I wanted to know how any given material does in a harsh environment."

Aitkaliyeva started a yearlong internship at Idaho National Laboratory in 2011 and joined the Nuclear Science User Facilities (NSUF) as a technical lead following her graduation in December 2012.

"The NSUF has played a large role in my life," she said. "It has helped me build my network, taught me how to write proposals, and design experiments. My students all had great experiences working with the NSUF. I credit NSUF with jump-starting my career. Having the ability to be able to do this work without having to pay for time is remarkable."

During her time as an NSUF technical lead, Aitkaliyeva's scientific work focused on understanding the behavior of plutonium-based fuels in contact with cladding materials. Her studies were designed to close the gap in the understanding of the progression of the fuel-cladding chemical interaction.

While working as a technical lead, Aitkaliyeva worked with various scientists to help them with preparing their proposals.

"I get to be the first one to look at the irradiated fuels and I get to do some really cool research," she said. "It's not that we are smarter than the people before us, it's just that we get to go back and look at the work and research and unravel more information. The NSUF really works to help conduct some of this research giving us access to state-of-the-art microscopes. The access they provide is unique."

Aitkaliyeva has authored more than 50 peer-reviewed journal publications and 90 presentations at professional meetings. She has published six peer reviewed journal papers based on her INL research. As a principal investigator, she has secured more than \$3.2 million in research funding for her work, including a \$593,000 grant for research equipment that benefits many others. She has received several awards and honors including the INL Early Career Award, Fuel Cycle Research and Development Excellence, Young Leaders Professional Development Award, Nuclear Engineering Science Teaching Award, and the U.S. Department of Energy's Early Career Award.

At the University of Florida, Aitkaliyeva's research group specializes in characterization of nuclear fuels and materials, with emphasis on establishing microstructure property relationships. She brought her fuels expertise to UF and established a facility dedicated to nuclear fuels and materials research. This facility is now part of NSUF and is available as part of rapid turnaround experiments.



### **Daniel Murray**

By Jeannette Boner

Daniel Murray is a materials research scientist and the group lead studying advanced ion characterization and micromechanics and surface analysis at Idaho National Laboratory. Murray's research interests include microstructural characterization of nuclear materials, in situ measurement of electronic and thermal properties of materials in the FIB, and nanostructured materials. Murray's research has led to a range of groundbreaking discoveries aimed at propelling advanced reactor technology forward.

"I have been given access to the focused ion beam (FIB) microscopes, and I have found unlimited potential for research," Murray said. "The Nuclear Science User Facilities program is a great resource for the study of materials science and nuclear energy. It allows us to get into the lab and gives us the ability to focus on the big issues while having the needed funding."

One of the research projects Murray and his team have worked to develop using the ion beam microscope is an accelerated process for advanced post irradiation examination. The process promises to shave years off the multidecade qualification cycle for nuclear fuels. This important effort will directly support the continued development of many of the advanced reactor concepts.

"When I first came to Idaho National Laboratory, I was heavily involved in the microscope program," he said. "It was then that I learned how time consuming analyses are and thought that we needed to develop methods that expedite the work we are doing. When you look at how quickly our nuclear energy technology is being developed, we need to keep up. One way to do this is by developing new methods for accelerating comprehensive characterizations of the microstructure and physical properties of irradiated fuels and materials and to provide higher quality correlated data."

The Irradiated Materials Characterization Laboratory (IMCL) is a 12,000 square foot facility located at Idaho National Laboratory's Materials and Fuels Complex. The hazard category 2 facility incorporates many features designed to allow researchers to safely and efficiently prepare and conduct microstructural level investigations on irradiated fuel.

IMCL focuses on microstructural. microchemical, and micromechanical analysis and thermophysical characterization of irradiated nuclear fuels. IMCL's unique design incorporates advanced characterization instruments that are sensitive to vibration, temperature, and electromagnetic interference into modular radiological shielding and confinement systems. The shielded instruments allow characterization of highly radioactive fuels and materials at the micro, nano, and atomic levels, the scale at which irradiation damage processes occur.

"With this current project funded by the Nuclear Science User Facilities, we are looking at 25 different samples of steels using one plate. We can complete an analysis in two days using the method in this project," he said. "This would normally take weeks or months. The FIB microscope provides a variety of data streams, so we put all the samples on at once, define the positions and just let it run. You come back two days later, and it's done."

"Normally, a post irradiation examination of materials uses a single purpose instrument and can provide incomplete characterization. Modern instrumentation with the capability for multimodal analysis and automation offers the potential to radically improve the rate at which characterization data can be acquired, the breadth of the data streams produced, and the correlation of data," Murray noted.

"Faster is better," Murray said.
"I'm tackling my part of the
post irradiation process by
shortening characterization
cycles and in turn, we can
shorten the overall process. In
the more advanced reactors,
which are very different from
the current fleet of light water
reactors, we either develop
new materials or we need
to be able to determine in a
quick manner if the current
materials will work. This is my
contribution to that."

Murray holds a doctorate in materials chemistry from the University of Nevada Reno. A California native and Idaho transplant, his sister is Kristin Zaitz, a founder of the nonprofit organization Mothers for Nuclear. She works at Diablo Canyon nuclear power plant in California, which their father helped build in the early 1970s.

As California's last remaining nuclear power plant, the facility is slated to be decommissioned by 2025.

"My family has a history in nuclear," Murray said. "I feel the urgency to develop and the importance of nuclear energy. Being in this profession, I want to work to help our energy sector. Nuclear is the best way to meet our climate goals."

"I come from a line of user facilities," Murray said. "It was so appealing to me to continue on in the user facility world, and that's why I pursued INL. User facilities attract researchers from all over the world, and we all are trying to tackle these problems together. Once I realized the full breadth of the FIB capabilities, it blew me away at the potential of what we can accomplish."



### Janelle Wharry

By Jeannette Boner

Janelle Wharry is an associate professor at Purdue University's School of Materials Engineering. Her research aims to understand structure-property-functionality relationships in irradiated materials.

"My research focuses on the effects of irradiation on materials," Wharry said. Her current projects span ferrous and non-ferrous structural alloys, reactor pressure vessel steels, model alloy

systems, electron beam welding, powder metallurgy with hot isostatic pressing alloys, and energy storage materials.

"I am particularly interested in the mechanical behavior of irradiated materials at the nano/microscale," she said.

Wharry, who has a doctorate in nuclear engineering and radiological sciences, said her work has been supported and elevated through access to the Nuclear Science User Facilities (NSUF). She considers the NSUF's Rapid Turnaround Experiment (RTE) award process as a defining opportunity to hone important grant writing skills. The streamlined process allowed her and her research team to focus on the critical work at hand.

"More than any other entity, the NSUF has enabled me to have an upward career trajectory," she said. "NSUF RTEs were the very first proposals I wrote and were awarded as a young assistant professor."

The RTE process offers researchers a framework to refine their proposal as it relates to performing irradiation effects studies of limited scope on nuclear fuels and materials utilizing NSUF facilities.

"Through RTEs, my students and I were able to obtain and publish meaningful, high quality data in a timely manner, which is difficult for junior faculty to do while building their own labs and before they land major grants," Wharry said. "This productivity with RTEs led to several invited talks at NSUF meetings, which further raised my group's profile and provided invaluable networking opportunities."

Wharry has had a number of RTE and Consolidated Innovative **Nuclear Research awards** supported by the NSUF. One particularly novel award on laser welding of irradiated steel highlighted how the NSUF supports dynamic and complex projects. The steel structures in nuclear reactors are exposed to high doses of radiation over their lifetimes, which in the most extreme cases can lead to cracking. To prevent a long term shutdown of the reactor, cracks are welded in irreplaceable structures. Unfortunately, when these weld repairs are returned to the reactor's harsh environment, the cracking is exacerbated. This happens because the heat from welding causes helium (which was generated in the steel during the original irradiation) to form into large bubbles, which worsens the cracking. "In our project, we looked at using laser welding as a possible solution, since laser welding injects lower amounts of heat into the

material than a conventional arc welding process," Wharry said. "This work was only possible because of the NSUF."

Wharry's team needed access to neutron irradiated steel to form the base material to make laser welds on the inside of a hot cell because of the material's radioactivity. This step could be completed at Westinghouse. Wharry then needed to characterize the laser welded specimens. This was done at the Center for Advanced Energy Studies. Ion irradiation of welds were completed at Texas A&M.

"All of this work at such unique facilities would have been unfeasible within the budget of a standard R&D grant or contract," Wharry said. "And the access to irradiated steel specimens was only made possible because of the NSUF's belief that valuable legacy and irradiated specimens should be competitively but equitably available to anyone in our research community."

Wharry's team demonstrated that laser welding could be used to effectively repair neutron-irradiated, helium containing steels, up to a modest level of helium content.

"This outcome means that within the nuclear power

industry, we now have a feasible, reliable method for repairing cracks in irreplaceable structural components," Wharry said. "This can help to further extend the lifetime of our current fleet of reactors which is particularly necessary as we face a climate crisis amidst nuclear plant shutdowns."

Wharry has published more than 70 peer reviewed journal articles and refereed conference papers. She is an editor of *Materials Today Communications* and serves on the editorial boards of two other materials journals. Seven papers were produced from the work the team did on the welding project.

"The nuclear materials research community is fortunate to have the NSUF as a resource, so we should do what we can as NSUF users to help support the program's longevity and funding by participating in NSUF supported conference sessions and contributing to NSUF reports and publicity," Wharry said.

Wharry has mentored 16 graduate/postdoctoral researchers and more than 50 undergraduate researchers. She also received the DOE Early Career Award, National Science Foundation CAREER Award, and American Nuclear Society (ANS) Landis Award.

Wharry credits the welding project with providing a learning and professional development opportunity for graduate student Keyou Mao. "He was able to build a strong professional network through collaborating closely with so many different scientists at numerous NSUF facilities," Wharry said. "He also received an NSUF RTE award to complement this work." She said these collective experiences set Keyou up for a successful career.

"He is currently transitioning from a postdoctoral position at Oak Ridge National Lab to an independent career as an assistant research professor," Wharry said. "This was made possible by the high scientific impact, professional references, and grant writing experience afforded him through this NSUF project."

Currently, Wharry serves as chair of the American Society for Testing and Materials Subcommittee E10.08 on Procedures for Radiation Damage Simulation; she was general chair of 2019 Materials in Nuclear Energy Systems (MiNES) Conference and former chair of the American Nuclear Society Materials Science & Technology Division.

### LABORATORY







Figure 1. (top) Activated Materials Laboratory nearing completion. (Middle) Initial rendering of the Activated Materials Laboratory.

### Supporting our nuclear future – The Activated Materials Laboratory

The Activated Materials Laboratory (AML) at the Advanced Photon Source (APS) will assist the nuclear community in examining radioactive samples utilizing High-Energy X-ray Microscope (HEXM) and other beamlines at the APS. This facility will support the broader needs of the nuclear community by introducing highly advanced X-ray characterization tools, providing more utility, and offering additional functions. Overall, the AML makes research more feasible and accessible to a larger community.

Placing the AML at Argonne
National Laboratory was an
ideal choice for many reasons.
The Nuclear Science User
Facilities (NSUF) encouraged this
decision because Argonne also
hosts the Irradiated Materials
Laboratory. This radiological
facility performs post irradiation
examination and specimen
preparation of radioactive
materials. It has been used for
irradiated sample receiving,
preparation, mounting and

disassembling in several APS experiments, including NSUF users. Additionally, Argonne operates the Intermediate Voltage Electron Microscopy-Tandem facility, a current NSUF partner facility.

The AML is critical due to growing interest in access to the most advanced synchrotron X-ray techniques for activated samples. Unfortunately, current challenges in sample transfer and handling create limitations. The AML will allow users to safely conduct experiments on radioactive materials and includes the capabilities to perform research without altering materials. Some additional benefits include minimal sample preparation; complex environments for in *situ* studies; and a wide range of scattering, imaging, and spectroscopy capabilities.

The main functions of the AML include (1) receiving and shipping activated samples; (2) exposing and processing open activated samples; (3)



characterizing, testing, and maintaining experimental apparatus for activated materials; and (4) temporary storage of activated samples before and after the experiment.

The design of the facility provides improved sample accessibility and flexible operation while minimizing the rotation time between samples. Altogether, this will enhance productivity and enable vast expansion of *in situ* testing capabilities.

High-energy X-rays interact with matter with low attenuation, small scattering angles and enhanced validity of the single-scattering approximation. These features, when combined with a source at high energies, make such X-rays the scattering probe of choice for nondestructively interrogating bulk material structure.

Recent developments in X-ray characterization shed new light on the mechanisms and pathways of microstructural evolution and its correlation with material's macroscopic behavior. The rapid advancement of 3D X-ray characterization tools is paving the way to a more complete understanding of microstructural heterogeneity and localized deformation of irradiated materials, critical to the prediction of material aging and degradation and the design of more irradiation-resistant materials.

While recent progress has demonstrated the great potential of synchrotron X-ray techniques for physical, chemical, and structural analysis of materials for nuclear energy applications, these techniques have not been made readily available to a broader nuclear scientific user community. This is primarily due to the limited access to suitable beamline facilities for handling radioactive samples. The AML will enable the nuclear community to investigate irradiated materials and nuclear fuels with a range

of synchrotron X-ray techniques that have robust radiological hazard and safety controls.

This facility will provide the NSUF with access to synchrotron radiation based examinations of materials with higher activation levels than are allowed in current beamline end stations. The NSUF has been able to provide funding for the design and construction of the AML. From FY 2020 to 2022, the NSUF has contributed approximately \$2.35 million toward the AML. The budget for AML includes the general construction costs, administration, management, testing and commissioning, as well as purchasing storage cabinets and gloveboxes for the laboratory.

With an estimated completion date of June 23, the NSUF is excited to support the AML and bring these important capabilities to our users.

# PROJECTS

### **Consolidated Innovative Nuclear Research**

Project Title	Principal Investigator	PI Organization	NSUF Facilities
Understanding Irradiation Behaviors of Ultrawide Bandgap Ga <sub>2</sub> O <sub>3</sub> High	Ge Yang	North Carolina State University	Center for Advanced Energy Studies
Temperature Sensor Materials for Advanced Nuclear Reactor Systems			North Carolina State University
Deployment and In-Pile Test of an Instrument for Real-Time Monitoring Thermal Conductivity Evolution of Nuclear Fuels	Zilong Hua	Idaho National Laboratory	Michigan Institute of Technology
Effect of Neutron Irradiation on Friction Stir Welded Ni-based ODS MA754 Alloy	Ramprashad Prabhakaran	Pacific Northwest National	Idaho National Laboratory
		Laboratory	Center for Advanced Energy Studies
			Pacific Northwest National Laboratory
ssessment of Irradiated Microstructure nd Mechanical Properties of FeCrAl Alloy abrication Routes	Andrew Hoffman	GE Research	Idaho National Laboratory
			University of Michigan



### Rapid Turnaround Experiments, 1st Call

Project Title	Principal Investigator	PI Organization	NSUF Facilities
Understanding Metallic Fuel Relocation Using Neutron Computed Tomography	Aaron Craft	ldaho National Laboratory	Idaho National Laboratory - Materials and Fuels Complex (MFC)
Microstructural Evolution in Model & Real RPV Steel Due to Thermal Aging and Low-Dose Irradiation Using Atom Probe Tomography	Benjamin Dacus	Massachusetts Institute of Technology	Center for Advanced Energy Studies - Microscopy and Characterization Suite (MaCS)
Irradiation of Stainless Steel Claddings Produced by Additive Manufacturing for In-core Applications	Burkan Isgor	Oregon State University	University of Wisconsin - Ion Beam Laboratory
IVEM Investigation of Defect Evolution in FCC Compositionally Complex Alloys Under Dual-beam Heavy-Ion Irradiation	Calvin Parkin	University of Wisconsin	Argonne National Laboratory — Intermediate Voltage Electron Microscope Tandem Facility (IVEM)
Assessing the Radial Thermal Conductivity Change in FBR MOX Fuel	Casey McKinney	University of Florida	Idaho National Laboratory - Materials and Fuels Complex (MFC)
Verifying Wigner Energy Measurements by <i>In-situ</i> TEM Annealing of Neutron-Irradiated Ti	Charles Hirst	Massachusetts Institute of Technology	Idaho National Laboratory - Materials and Fuels Complex (MFC)
Defect Generation and Phase Stability in Single Crystal Mixed Uranium-Thorium Actinide Oxides	Cody Dennett	Idaho National Laboratory	Center for Advanced Energy Studies - Microscopy and Characterization Suite (MaCS) and University of Michigan - Michigan Ion Beam Laboratory (MIBL)

Project Title	Principal Investigator	PI Organization	NSUF Facilities
Microstructural Examination of Irradiation Effects on Metal Matrix Composite Neutron Absorber	Donna Guillen	ldaho National Laboratory	Center for Advanced Energy Studies - Microscopy and Characterization Suite (MaCS)
Radiation-induced Crystallization in Alumina Coatings: Temperature and Yttria Doping Effect. A Completion Kinetic Study to Model Radiation Resistant Coatings for the Future Nuclear System.	Fabio Di Fonzo	lstituto Italiano di Tecnologia	Argonne National Laboratory — Intermediate Voltage Electron Microscope Tandem Facility (IVEM)
Study of Minor Actinides Redistribution and Fission Products in High Burnup MOX Using Electron Probe Micro Analysis (EPMA)	Fabiola Cappia	Idaho National Laboratory	Idaho National Laboratory - Materials and Fuels Complex (MFC)
The Effects of Stress on Void Superlattice Formation During Cr+ Self-Ion-Irradiation of Chromium	Francis Garner	Texas A&M University	Center for Advanced Energy Studies - Microscopy and Characterization Suite (MaCS) and Texas A&M University - Accelerator Laboratory
Effect of Neutron Radiation on Density and Mechanical Properties of Concrete Aggregates	Ippei Maruyama	Nagoya University	Oak Ridge National Laboratory - Low Activation Materials Development and Analysis (LAMDA)
Mechanistic Insight Through TEM Characterization of Intergranular Irradiation-Assisted Stress Corrosion Crack Tips in As-Irradiated vs. Post-Irradiation Annealed Specimens	Jean Smith	Electric Power Research Institute	Idaho National Laboratory - Materials and Fuels Complex (MFC)

### Rapid Turnaround Experiments, 1st Call

Project Title	Principal Investigator	PI Organization	NSUF Facilities
Imaging of Irradiation Effects in Tantalum Alloys for Fast-Spectrum Self-Powered Neutron Detectors	Kathleen Goetz	University of Tennessee-Knoxville	Oak Ridge National Laboratory - Low Activation Materials Development and Analysis (LAMDA)
Computational Thermochemistry of Pathways Toward Synthesis of Uranium Nitride	Michael Miller	Southwest Research Institute	Idaho National Laboratory - Materials and Fuels Complex (MFC)
Heavy Ion Irradiation and Characterization of Light-Refractory, BCC High-Entropy Alloys	Michael Moorehead	University of Wisconsin	University of Wisconsin - Ion Beam Laboratory
In-situ Mechanical Testing of Neutron- Irradiated 304SS Exhibiting Unusual Deformation and Fracture Behavior with Respect to Temperature	Mike Burke	Electric Power Research Institute	University of California- Berkeley - Nuclear Materials Laboratory and Westinghouse Churchill Laboratory Services
Correlative TEM and APT Approach to Elucidate Hydride Morphology and Behavior in Ex-Service Pressure Tube Material	Mukesh Bachhav	Idaho National Laboratory	ldaho National Laboratory - Materials and Fuels Complex (MFC)
Changes in Mechanical and Chemical- Structural Properties of Gamma Irradiated Calcium Silicate Hydrates to an Absorbed Dose of 189 MGy with Respect to Pristine Samples Subjected to the Same Temperature History	Nishant Garg	University of Illinois at Urbana-Champaign	Oak Ridge National Laboratory - Low Activation Materials Development and Analysis (LAMDA)
The Sink Strength and Radiation Parameter Effects on Microchemical Evolution in Dual- Ion Irradiated Additively Manufactured and Wrought HT9	Pengyuan Xiu	University of Michigan	Center for Advanced Energy Studies - Microscopy and Characterization Suite (MaCS)
Comparison of Solute Cluster Formation and Evolution in Neutron-Irradiated ATR-2 to Thermally-Aged Low-Alloy Steels	Przemysław Klups	University of Oxford	Center for Advanced Energy Studies - Microscopy and Characterization Suite (MaCS)
Ion Irradiation and Examination of Additive Friction Stir Manufactured 316 Stainless Steel Component	Rajiv Mishra	University of North Texas	Center for Advanced Energy Studies - Microscopy and Characterization Suite (MaCS) and Texas A&M University - Accelerator Laboratory

Project Title	Principal Investigator	PI Organization	NSUF Facilities
Microstructural Characterization of Neutron Irradiated NF616 (Grade 92) as a Function of Doses and Temperatures	Ramprashad Prabhakaran	Pacific Northwest National Laboratory	Pacific Northwest National Laboratory - Materials Science and Technology Laboratory
lon Irradiation and Examination of 304 Stainless Steel and 304 ODS Steel Additively Manufactured via Selective Laser Melting	Somayeh Pasebani	Oregon State University	Center for Advanced Energy Studies - Microscopy and Characterization Suite (MaCS) and Texas A&M University - Accelerator Laboratory
The Role of Precipitate Coherency on Helium Trapping in Additively Manufactured Alloy 718	Stephen Taller	Oak Ridge National Laboratory	Oak Ridge National Laboratory - Low Activation Materials Development and Analysis (LAMDA) and University of Michigan - Michigan Ion Beam Laboratory (MIBL)
Local Thermal Properties of Fast Reactor MOX Fuels	Troy Munro	Brigham Young University	Idaho National Laboratory - Materials and Fuels Complex (MFC)
Pre-Oxidation Effect on ATF Cladding Performance by Characterization of Irradiated FeCrAl-UO <sub>2</sub> Capsules	Vipul Gupta	General Electric Global Research	Oak Ridge National Laboratory - Low Activation Materials Development and Analysis (LAMDA)
A First Investigation in Lanthanide-Induced Grain Boundary Embrittlement in HT9 Cladding via <i>In-situ</i> Micro-Tensile Testing	Yachun Wang	Idaho National Laboratory	Idaho National Laboratory - Materials and Fuels Complex (MFC)
Coupling CFD and ML to Transform the Coated Nuclear Fuels Fabrication Process	Zachary Mills	Oak Ridge National Laboratory	Idaho National Laboratory - Materials and Fuels Complex (MFC)



# REPORTS

hrough its RTE and CINR calls for proposals, NSUF grants access to its facilities for researchers to conduct their studies to further the understanding of the effects of irradiation on nuclear fuels and materials. The following reports resulted from these NSUF projects.

#### **Technical Reports**

*In Situ* Ion Irradiation to add Irradiation Assisted Grain Growth to the Marmot Tool

#### **Short Communications**

Ion Irradiation for High Fidelity Simulation of High Dose Neutron Irradiation

Bubble formation of *In situ* He-implanted 14YWT and CNA Advanced Nanostructured Ferritic Alloys

Changes in Mechanical and Chemical-Structural Properties of Gamma Irradiated Calcium Silicate Hydrates to an Absorbed Dose of 200 MGy with Respect to Pristine Samples

In Situ SEM Irradiation Enhanced Creep Studies of 14 YWT

Ion Irradiation of ThO<sub>2</sub> and UO<sub>2</sub> Single Crystals

Defect Clustering in 316H Stainless Steel and High Entropy Alloy Under *In-situ* Irradiation at 600-700°C

Atom Probe characterization of Neutron Irradiated Commercial ZIRLO® and AXIOM X2® Alloys

### TECHNICAL REPORT

## In Situ Ion Irradiation to add Irradiation Assisted Grain Growth to the Marmot Tool

Arthur Motta - Pennsylvania State University - atm2@psu.edu



ost studies of grain growth in UO<sub>2</sub> are based on thermally driven processes at elevated temperatures. However, studies have shown that grain growth can occur even at cryogenic temperatures by ballistic processes. Such irradiation induced grain growth in UO<sub>2</sub> has yet to be studied. Advanced in situ Kr ion irradiation and Transmission Electron Microscopy (TEM) were systematically performed on nanocrystalline UO<sub>2</sub> thin films at temperatures ranging from 50 K to 1073 K; grain growth was observed at all temperatures. A combination of manual and machine learning techniques was used to measure and plot grain-size evolution against irradiation fluence at various irradiation temperatures. Data was fitted using classical grain growth and thermal spike models. The impact of irradiation on grain growth was also implemented in MARMOT.

#### Introduction

In the Nuclear Energy Advanced Modeling and Simulation (NEAMS) program, the MARMOT mesoscale fuel performance tool is used to inform the development of mechanistic materials models for the BISON fuel performance tool. The grain size of the fuel has a large impact on its performance, directly impacting heat conduction, fission gas release, creep, and fracture. Thus, atomistic and mesoscale MARMOT simulations have been used to investigate grain boundary migration and grain growth in  $UO_2$  [1–2]. The mechanism for steady state thermal grain growth is the migration of individual grain boundaries to reduce the overall energy of the system, such that concave boundaries recede and convex boundaries advance. This results in the growth of some grains at the expense of the shrinkage and disappearance of other grains. In addition to thermal mechanisms, grain growth

has also been observed due to irradiation in both experiment [3] and simulation [4]. Grain growth resulting from irradiation is usually found to occur at a higher rate than thermal growth at intermediate temperatures. The motion of grain boundaries and growth of grains is commonly attributed to the thermal spikes that occur during the irradiation damage process. These "high temperature" spikes cause many atomic jumps. When a thermal spike overlaps one or more grain boundaries, a bias in atomic transport across the grain boundary caused by its curvature results in grain boundary migration and grain growth. The current grain growth model in MARMOT only considers grain growth kinetics of fresh, unirradiated fuel. Thus, it may be missing a crucial mechanism that could significantly hurt the accuracy of its predictions. The objectives of this project are twofold. First, the effects of irradiation on grain growth

Fuel performance models must consider the effects of irradiation on the  $UO_2$  grain growth.

of UO<sub>2</sub> was experimentally investigated under various conditions and as a function of grain size. The impacts of isothermal annealing temperature and irradiation on grain growth kinetics were quantified in thin film UO<sub>2</sub> TEM samples using in situ techniques. Second, using the data obtained, the capabilities of the MARMOT tool have been expanded to account for the effects of irradiation on grain growth. The experimental data is being used to validate simulations run using MARMOT. Once complete, the expanded MARMOT capabilities will be used to assess the effects of irradiation on grain growth in light water reactor fuel pellets.

#### **Project Hypothesis**

In the NEAMS program, the MARMOT code is used to inform the development of models for the BISON fuel

performance tool. The fuel's grain size has a large impact on its performance. However, the current grain growth model in MARMOT only considers grain growth kinetics of fresh, unirradiated fuel. This work is to experimentally study irradiation effects on grain growth in UO2 and implement these effects into MARMOT. This work is being performed using coincident and synergistic efforts of experiment and simulation. *In situ* TEM experiments were performed at the Intermediate Voltage Electron Microscopy (IVEM) Nuclear Science User Facilities (NSUF) partner facility at Argonne National Laboratory to study grain growth in both isothermal annealing and ion irradiation conditions.

# Experimental or Technical Approach

The UO<sub>2</sub> samples were synthesized by pulsed laser deposition at Los Alamos National Laboratory. About 30 to 50 nm thick UO<sub>2</sub> thin films were deposited on SiN wafers, which contained an electron transparent window at the center. The samples were irradiated with 1 MeV Kr ions at the IVEM at temperatures ranging from 50 K to 1073 K. The ion dose rate of 6.25 x 10<sup>12</sup> ions/cm<sup>2</sup>/s corresponds to a total of over 10<sup>15</sup> ions/ cm<sup>2</sup> for the irradiation times used. Isothermal annealing experiments without irradiation were also conducted using the same TEM sample holder. The samples were characterized by systematically taking brightfield and dark-field images during irradiation as well as diffraction patterns. The quantified results on grain diameters at all temperatures and all fluences have been analyzed by using a manual and a machine learning method. The machine learning method utilized a U-Net architecture, which has a unique U-shaped architecture with a contracting path to extract image context and a symmetric expansive path to propagate context information to higher resolution layers [5]. An NVIDIA Tesla P100

GPU was used to train the model to 200 epochs with L2 Regularization. The training was terminated when the validation loss became stable. The total training time was about 6 hours.

The impact of irradiation was added to the existing UO<sub>2</sub> grain growth model in MARMOT [1, 2] by coupling it with a model of heat conduction in UO<sub>2</sub>. Thermal spikes were added to the system by explicitly representing heat generation in the heat equation:

$$\rho C_P \frac{\partial T}{\partial t} = \nabla (k \nabla T) + \dot{q} ,$$

where  $\partial T/\partial t$  is the rate of change of the temperature field T, k is the thermal conductivity, q is the volumetric heat generation term,  $\rho$  is the density, and  $C_p$  is the specific heat capacity. The heat generation term varied in time and space to account for the thermal spikes. When and where a thermal spike occurred in the domain was determined randomly. The spikes were defined by the magnitude of the heat source during a spike, the average rate at which the spikes occur in units of spikes per second per unit volume (a function of the fluence), the radius of the area over which

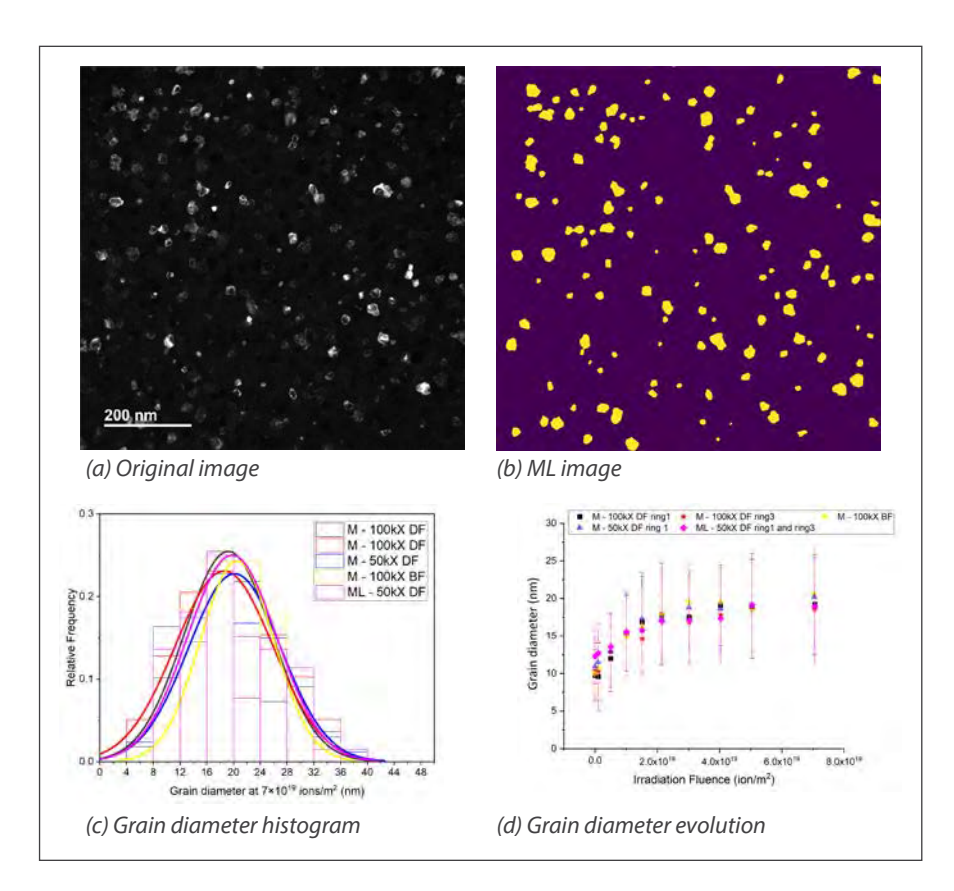


Figure 1. (A) Original 50xK DF TEM image showing the grain (in white contrast) of 50 K irradiated sample. (B) ML generated image showing the identified grains in yellow. (C) Comparison of the grain-size distribution at a fluence of around 7×10<sup>19</sup> ions/m² using the M and ML methods. (D) Average grain diameter as a function of irradiation fluence. The errors are the standard deviation of measured grain diameters.

the heat is applied, and the length of time over which the heat source is maintained or the hold time. The values for these quantities were set to mimic the ion irradiation conditions used in the *in situ* experiments.

In this coupled model, the impact of irradiation is added via temperature changes due to thermal spikes. The thermal spikes cause the local temperature to increase, increasing the grain boundary mobility. This results in local grain boundary migration. The grain growth and heat-conduction models were

fully coupled and solved simultaneously using an implicit finite element approach in MARMOT.

#### **Results**

Experimental Results
The major measurement in this project is the average grain diameter, determined by manual (M) and machinelearning (ML) methods. The M measurements were performed on both dark-field (DF) and bright-field (BF) TEM images at different magnifications to improve the statistics. ML measurements were only performed on 50 kX DF TEM images. Figure 1 compares the

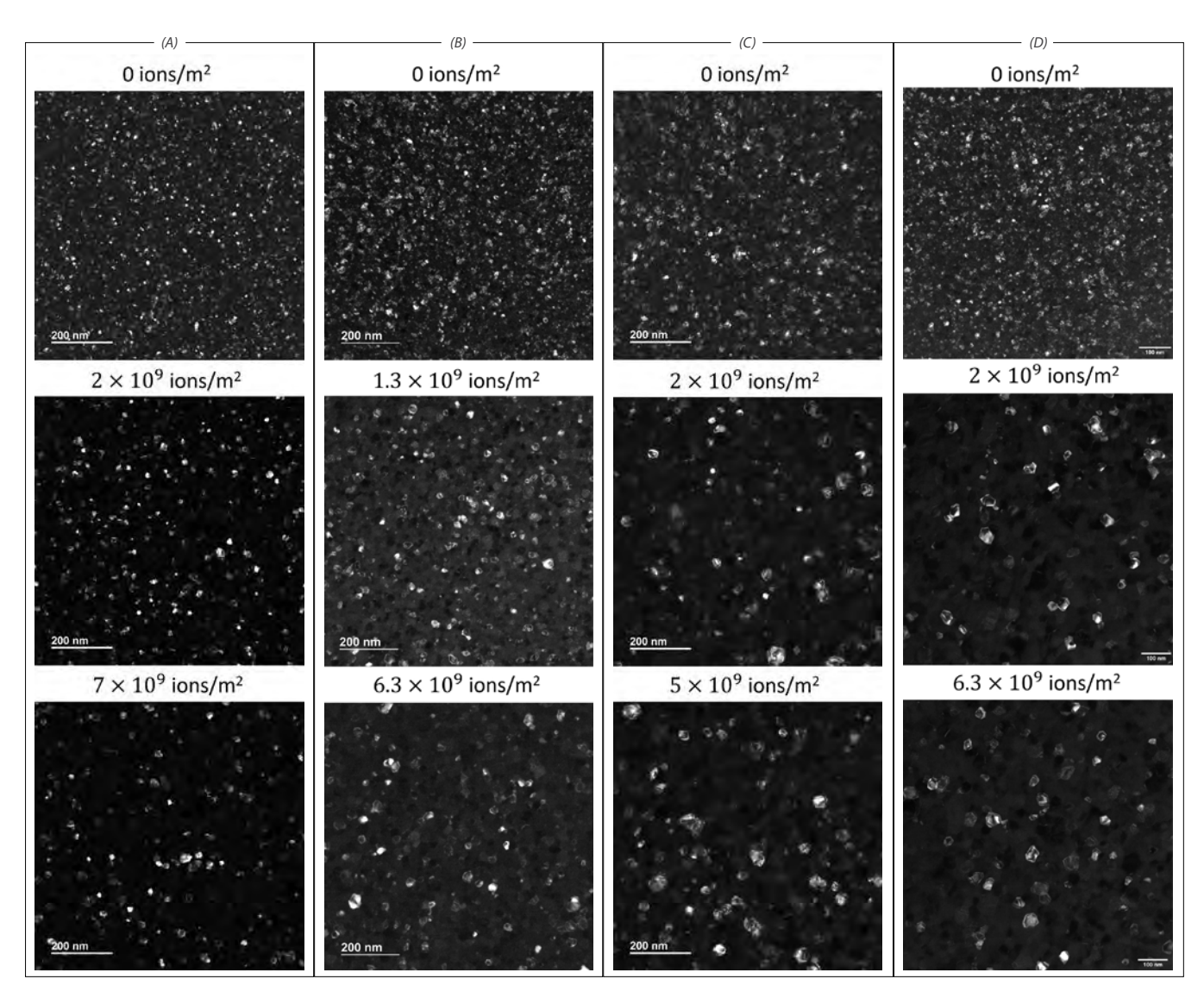
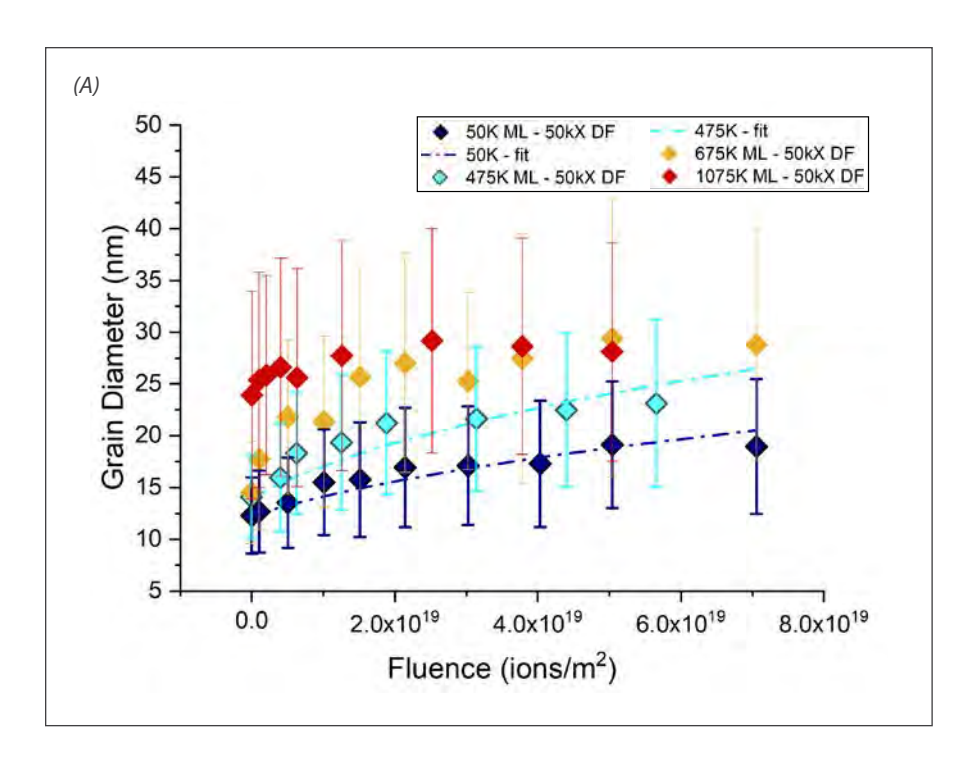


Figure 2. 50-xK DF TEM images showing the grain growth at (A) 50 K, (B) 475 K, (C) 675 K, and (D) 1075 K irradiation temperature up to  $7 \times 10^9$  ions/m<sup>2</sup>.



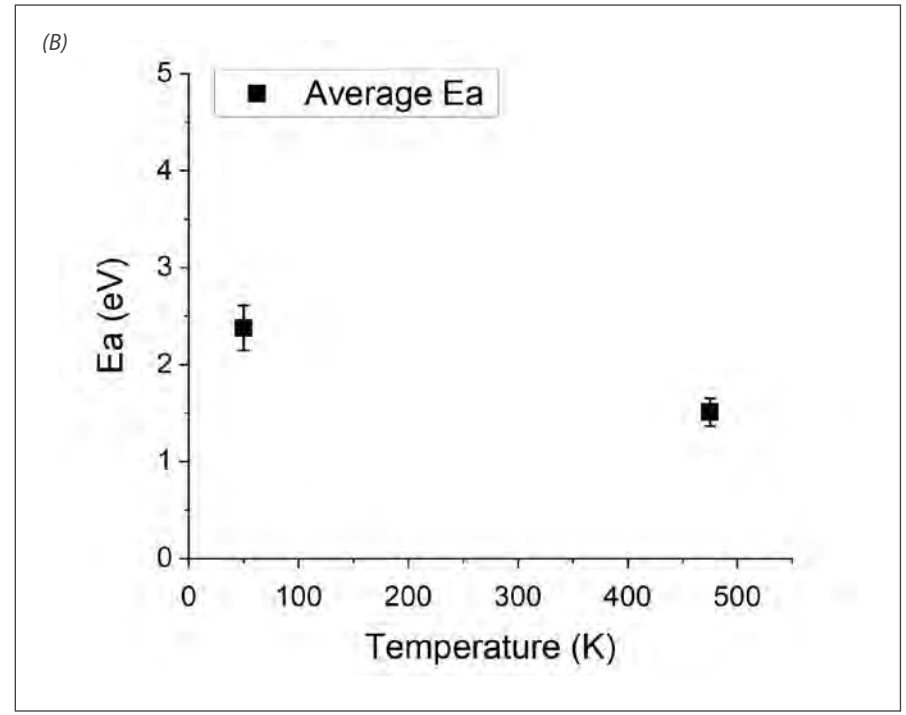


Figure 3. (A) Grain diameter evolution plot as a function of irradiation fluence at different irradiation temperatures. The errors are the standard deviation of measured grain diameters. (B) Calculated activation energy ( $E_{\rm a}$ ) for grain growth at 50 K and 475 K, respectively.

grain diameters measured by M and ML methods, respectively. The two methods show great consistency. The grain diameter evolution as a function of irradiation fluence at 50 K is also plotted in Figure 1 D. There is clear grain growth at 50 K under irradiation. Thermally driven grain growth would not occur at this temperature; therefore, the grain growth observed is purely an irradiation effect.

In addition to the 50 K irradiation experiments, additional studies were performed on  $\rm UO_2$  samples at higher temperatures. Figure 2 shows TEM images of sample irradiated at different temperatures. Qualitatively, the grain diameters appear to become much larger at higher doses for all temperatures. The grain diameters at higher irradiation temperature at 675 K and 1075 K are much larger than lower irradiation temperatures at 50 K and 475K.

A quantitative analysis on the grain growth kinetics was carried out, and the results are shown in Figure 3 (A). The grain growth at 675 K and 1075 K results from a combination of irradiation and thermally assisted processes; therefore, these grain growths were not analyzed. The data at 50 K and 475 K were fitted to a grain growth equation based on the thermal spike model [3].

The fitting equations are as follows:

$$D^3-D_0^3=K\phi t$$

(2) 
$$K = \frac{36\gamma d_{spike} X \delta V_{at^{V}} \sqrt{\frac{3}{5}} \Gamma(\frac{8}{3}) k_{B}^{\frac{5}{3}}}{10\pi C_{0}^{\frac{2}{3}} k_{0}} \frac{Q^{\frac{5}{3}}}{(E_{a}^{spike})^{\frac{8}{3}}}$$

where  $D_0$  is the initial grain diameter,  $\phi$  is the ion flux (ions/m²/s), t is time (s), and K is the growth rate (nm³/[ions/m²]), which is obtained by fitting Eq. (1) to the measured grain diameters. Other variables are described in Table 1. From Eq. (2),  $E_a$  can be calculated and is shown in Figure 3 (B) for two different temperatures. At 50 K, the  $E_a$  is about 2.5 eV, whereas it is about 1.5 eV at 475 K. However,  $E_a$  should be a temperature independent parameter. If data at 675 K and 1075 K were fitted to Eqs. (1) and (2), the calculated  $E_a$  would be even smaller. This is because Eq. (2) is only valid for low temperature irradiation,

where there is no thermally assisted grain growth.

To evaluate the thermal effect on the grain growth, isothermal annealing experiments without irradiation were also performed. Both M and ML results are plotted in Figure 4. Only the annealing temperature higher than 475 K resulted in grain growth and grain growth started to plateau after about 2 hours. These data are fitted to two different thermal grain growth equations as following:

Figure 4. Grain diameter evolution under isothermal annealing.

$$D^n - D_0^n = Mt$$

(4) 
$$\frac{dD}{dt} = A\left(\frac{1}{D} - \frac{1}{D_{\text{max}}}\right)$$

where D is the measured average grain diameter,  $D_0$ is the initial average grain diameter, *n* is the growth rate exponent, M is a kinetic parameter, t is the annealing time,  $D_{max}$  is the measured maximum grain diameter, and A is another kinetic parameter similar to M. In Eq. (3), the values of n and M are fit to the data and in Eq. (4), the values of A and  $D_{max}$  are fit. For Eq. (3), n has to be greater than 10 to capture the plateau region, which is very high compared to other UO<sub>2</sub> data. Eq. 4

Parameters	Variables	Values
Average grain boundary energy	γ	1 (J/m²)
Thermal spike diameter	$d_{spike}$	9.63 (nm)
Thermal spikes per ion	X	0.0407 (spikes/ion/nm)
Grain boundary width	δ	0.6 (nm)
Atomic volume	$V_{at}$	0.0136 (nm³/atm)
Debye frequency	v	2.20 (THz)
Boltzmann constant	$k_B$	8.62×10 <sup>-5</sup> (eV/K)
Average thermal spike energy	Q	25.27 keV
Heat capacity	$C_0$	213.96 (J/mol/K)
Thermal conductivity	$k_0$	3 (W/m K)

Table 1. The description and literature values of the variables needed to calculate the thermal spike grain growth kinetic parameter K [6-31].

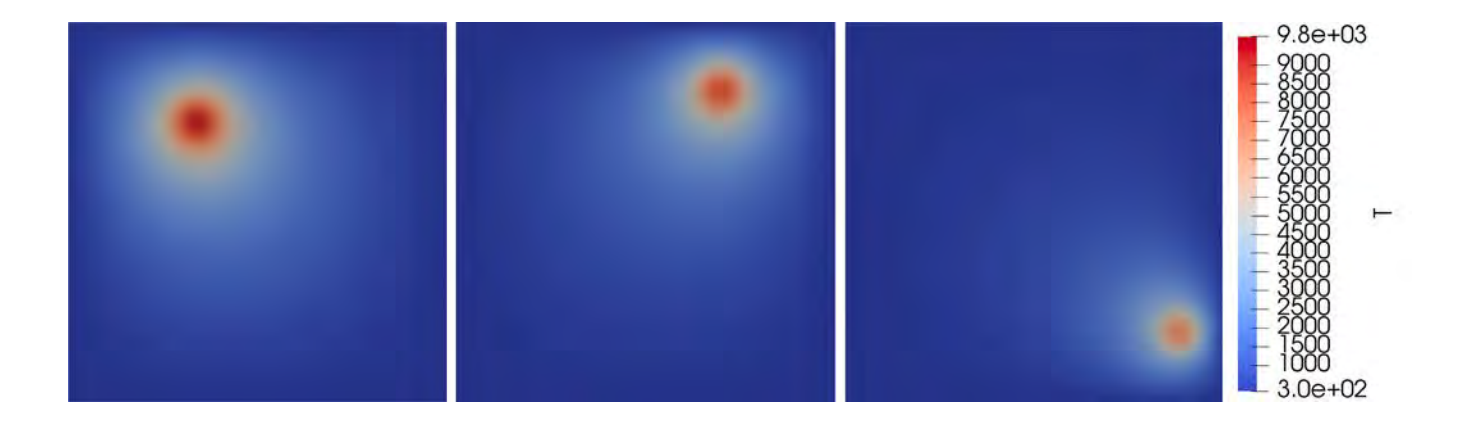


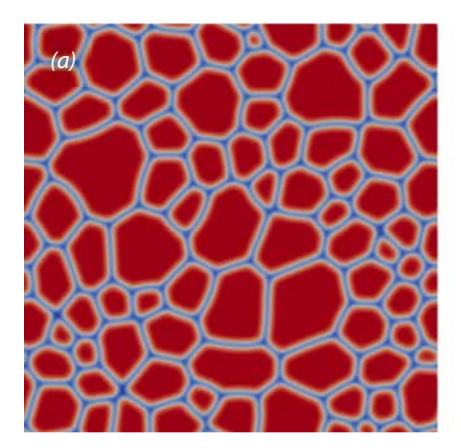
Figure 5. Simulation results with just heat conduction, where thermal spikes occur at random times and locations within the 300 × 300 nm domain. The temperature profile is shown after three different random spike events.

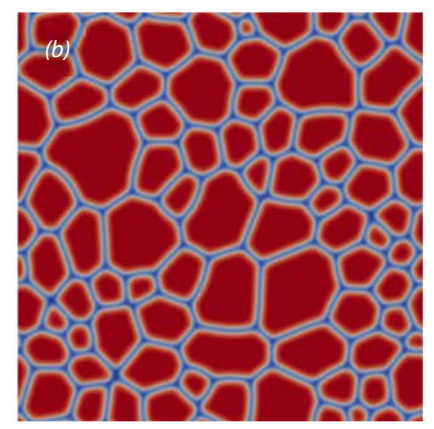
captures the plateau region well. By using a parameter described in [10] to obtain the A parameter, the activation energy (Q) for thermal grain growth is calculated to be 2.45 eV, which is consistent to our previously calculated  $E_a$  based on the thermal spike model and is similar to what has been found for other  $UO_2$  grain growth data [1].

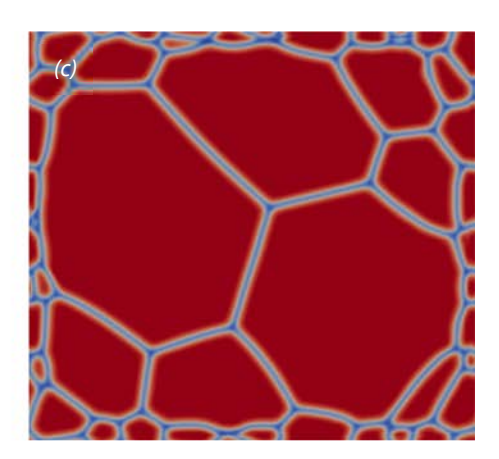
**MARMOT Model Results** To test the behavior of thermal spikes in the heat conduction model, it was run separately from the grain growth model. A  $30 \times 30$  nm 2D domain of UO<sub>2</sub> was simulated during irradiation with 1 MeV Kr ions at 300 K. The temperature at the domain boundaries was fixed at 300 K to represent the heat sink around the sample. The temperature profile after various thermal spikes is shown in Figure 5. The temperature gets very large within the thermal spike, reaching nearly 10,000

K. However, after the thermal spike, the heat quickly dissipates throughout the domain and the domain returns to 300 K. The temperature is higher in thermal spikes further from the boundaries then in spikes that are near the boundaries.

Grain growth at 300 K was then modeled in a  $30 \times 30$  nm 2D domain with and without ion irradiation. A grain structure was generated with an average grain size of 4 nm, shown in Figure 6(a), similar to the average grain size in the UO<sub>2</sub> thin films used in the ion irradiation experiments. Grain growth was modeled for 5000 s. Without irradiation, the final microstructure, shown in Figure 6(b), was identical to the initial grain structure. This is consistent with the thermal grain growth experiments, in which grain growth did not occur in temperatures below 475 K. With irradiation, the coupled grain growth and heatconduction model that included







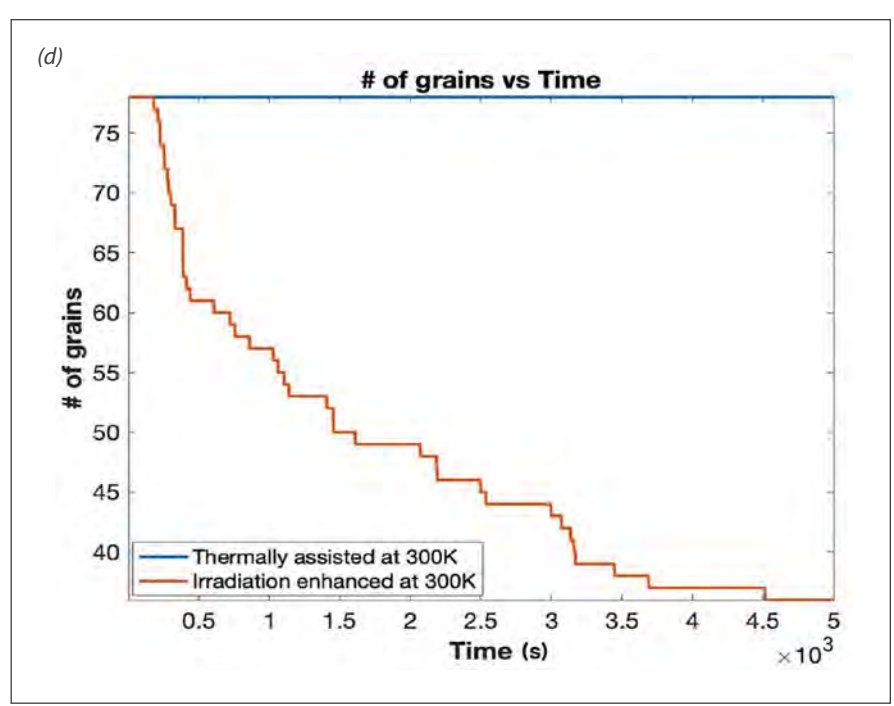


Figure 6. Comparison of grain growth with and without ion irradiation simulated using MARMOT in a  $300 \times 300$  nm domain at 300 K. (a) The initial grain structure; (b) and (c) the grain structure after 5000 s without and with irradiation, respectively. (d) The number of grains versus simulation time. In (a-c), grains are shown in red and grain boundaries in blue.

the thermal spikes predicted a large amount of grain growth as shown in Figure 6(c). The grains grew quickly away from the boundaries; however, near the boundaries, much less grain growth occurred due to the fixed 300 K temperature at the boundaries. The number of grains went from 77 in the initial structure to 46 after 5000 s, as

shown in Figure 6(d).

#### **Discussion**

This work builds directly on work that is already completed or underway for the NEAMS program. The current status and data needs of MARMOT align well with this research. *In situ* TEM characterization has provided initial and final

microstructures, per grain size and well controlled experimental conditions that are all desirable for MARMOT validation data. In particular, the grain growth data of nanocrystalline samples is desired, including both "annealing of well characterized microstructures" and "grain growth under irradiation," both of which have been achieved with the in situ TEM experiment. This work has also enhanced the capabilities of MARMOT, adding the impact of thermal spikes on grain growth. The new data will be used to validate the new MARMOT capability. While the design of this in situ experiment requires conditions atypical of those in reactor, the underlying science is the same and advancements made with these experiments are applicable to in reactor conditions. In fact, once the model in MARMOT has been fully developed and validated, it will be used to assess the impact of irradiation on UO<sub>2</sub> grain microstructure at light water reactor (LWR) conditions and if this effect should be included in the BISON fuel performance tool.

#### **Conclusion**

The impact of irradiation on grain growth in UO<sub>2</sub> was investigated using ion irradiation. This effect was also added to the MARMOT tool. Grain growth under irradiation occurred even at 50 K; higher irradiation temperatures led to gradually increasing grain growth rates. The calculated activation energy (E<sub>a</sub>) for irradiation induced grain growth based on the thermal spike model was about 2.5 eV. The isothermal annealing results show the grains only start to grow at temperature higher than 475 K. The calculated thermal activation energy (Q) based on classical thermal grain growth equation with extra resistive force provide a similar activation energy. At temperature greater than 475 K in irradiated samples, grain growth occurred due to both thermal and irradiationenhanced grain growth. The MARMOT UO<sub>2</sub> grain growth model was coupled to a heatconduction model, including thermal spikes, and the resultant model predicted no thermal grain growth at 300 K but significant irradiation enhanced grain growth.

#### **Future Activities**

The primary remaining goal for this project is to validate the irradiation enhanced grain

growth model in MARMOT. The temperatures and irradiation conditions used in the in situ experiments will be duplicated in grain growth simulations with many more grains and for longer times than the simulation shown in Figure 6. The results from the model will be directly compared with the data and the model accuracy will be assessed. The validated MARMOT model will then be used to determine if irradiation enhanced grain growth needs to be included in the BISON grain growth model.

#### References

- [1.] M. R. Tonks, P. C. A. Simon, J. Hirschhorn. "Mechanistic grain growth model for fresh and irradiated UO<sub>2</sub> nuclear fuel." J. Nucl. Mater. 543 (2021) 152576. https://doi.org/10.1016/j. jnucmat.2020.152576.
- [2.] R.T. Michael, Z. Yongfeng, B. Aaron, B. Xian-Ming. "Development of a grain boundary pinning model that considers particle size distribution using the phase field method." Model. Simul. Mater. Sci. Eng. 23 (2015) 45009. http://stacks.iop.org/0965-0393/23/i=4/a=045009.

- [3.] D. Kaoumi, A. T. Motta, R. C. Birtcher. "A thermal spike model of grain growth under irradiation." J. Appl. Phys. 104 (2008) 1–13. https://doi. org/10.1063/1.2988142.
- [4.] W. Voegeli, K. Albe, H. Hahn. "Simulation of grain growth in nanocrystalline nickel induced by ion irradiation." Nucl. Instruments Methods Phys. Res. Sect. B Beam Interact. with Mater. Atoms. 202 (2003) 230–235. https://doi.org/10.1016/S0168-583X(02)01862-1.
- [5.] O. Ronneberger, P. Fischer, T. Brox. "U-net: Convolutional networks for biomedical image segmentation." *Lect. Notes Comput. Sci.* (Including Subser. Lect. Notes Artif. Intell. Lect. Notes Bioinformatics). 9351 (2015) 234–241. https://doi.org/10.1007/978-3-319-24574-4\_28.
- [6.] P. S. Maiya. "Surface diffusion, surface free energy, and grainboundary free energy of uranium dioxide."

  J. Nucl. Mater. 40 (1971) 57–65. https://doi.org/10.1016/0022-3115(71)90116-4.

- [7.] E. N. Hodkin, M. G. Nicholas. "Surface and interfacial properties of non-stoichiometric uranium dioxide." *J. Nucl. Mater.* 67 (1977) 171–180. https://doi.org/10.1016/0022-3115(77)90172-6.
- [8.] P. Nikolopoulos, S. Nazaré, F. Thümmler. "Surface, grain boundary and interfacial energies in UO<sub>2</sub> and UO<sub>2</sub>-Ni." J. Nucl. Mater. 71 (1977) 89–94. https:// doi.org/10.1016/0022-3115(77)90191-X.
- [9.] P. V. Nerikar, K. Rudman, T.G. Desai, D. Byler, C. Unal, K. J. McClellan, S. R. Phillpot, S. B. Sinnott, P. Peralta, B. P. Uberuaga, C. R. Stanek. "Grain boundaries in uranium dioxide: Scanning electron microscopy experiments and atomistic simulations." J. Am. Ceram. Soc. 94 (2011) 1893–1900. https://doi.org/10.1111/j.1551-2916.2010.04295.x.
- [10.] Y. Zhang, P. C. Millett, M. R. Tonks, X. M. Bai, S. B. Biner. "Molecular dynamics simulations of intergranular fracture in UO<sub>2</sub> with nine empirical interatomic potentials." J. Nucl. Mater.

- 452 (2014) 296–303. https://doi.org/10.1016/j. jnucmat.2014.05.034.
- [11.] E. Bourasseau, A. Mouret, P. Fantou, X. Iltis, R.C. Belin, Experimental and simulation study of grain boundaries in UO<sub>2</sub>, *J. Nucl. Mater.* 517 (2019) 286–295. https://doi.org/10.1016/j. jnucmat.2019.02.033.
- [12.] A. Ksibi, E. Bourasseau, X. Iltis, D. Drouan, M. Gaudet, A. Germain, A. Pena, G. Lapertot, J. P. Brison, R. C. Belin, "Experimental and numerical assessment of grain boundary energies in polycrystalline uranium dioxide." *J. Eur. Ceram.*Soc. 40 (2020) 4191–4201. https://doi.org/10.1016/j. jeurceramsoc.2020.04.041
- [13.] C.J. Ulmer, W. Y. Chen, D. E. Wolfe, A. T. Motta. "In-situ ion irradiation induced grain growth in nanocrystalline ceria." J. Nucl. Mater. 545 (2021) 152688. https://doi.org/10.1016/j.jnucmat. 2020.152688.
- [14.] T. G. Godfrey, W.
  Fulkerson, T. G. Kollie, J
  .P. Moore, D. L. McElroy.
  "Thermal Conductivity of
  Uranium Dioxide from

- -57° to 1100°C by a Radial Heat Flow Technique." *J. Am. Ceram. Soc.* 48 (1965) 297–305. https://doi. org/10.1111/j.1151-2916.1965.tb14745.x.
- [15.] T. K. Engel, The heat capacities of Al<sub>2</sub>O<sub>3</sub>, UO<sub>2</sub> and PuO<sub>2</sub> From 300 To 1100 °K, *J. Nucl. Mater.* 31 (1969) 211–214. https://doi.org/10.1016/0022-3115(69)90194-9.
- [16.] F. Grønvold, N. J. Kveseth, A. Sveen, J. Tichý.

  "Thermodynamics of the UO<sub>2+x</sub> phase I. Heat capacities of UO<sub>2.017</sub> and UO<sub>2.254</sub> from 300 to 1000 K and electronic contributions." *J. Chem. Thermodyn.* 2 (1970) 665–679. https://doi.org/10.1016/0021-9614(70)90042-X.
- [17.] J. J. Huntzicker, E. F. Westrum. "The magnetic transition, heat capacity, and thermodynamic properties of uranium dioxide from 5 to 350 K." J. Chem. Thermodyn. 3 (1971) 61–76. https://doi.org/10.1016/S0021-9614(71)80067-8.

- [18.] H. Inaba, K. Naito, M. Oguma. "Heat capacity measurement of  $U_{1-y}Gd_yO_2$  (0.00  $\leq y \leq$  0.142) from 310 to 1500 K." J. Nucl. Mater. 149 (1987) 341–348. https://doi.org/10.1016/0022-3115(87)90536-8.
- [19.] Y. Takahashi, M. Asou. "High-temperature heat-capacity measurements on (U, Gd)O<sub>2</sub> by drop calorimetry and DSC." *J. Nucl. Mater.* 201 (1993) 108–114. https://doi.org/10.1016/0022-3115(93)90164-T.
- [20.] C. Ronchi, M. Sheindlin, M. Musella, G. J. Hyland. "Thermal conductivity of uranium dioxide up to 2900 K from simultaneous measurement of the heat capacity and thermal diffusivity." J. Appl. Phys. 85 (1999) 776–789. https://doi.org/10.1063/1.369159.
- [21.] P. Goel, N. Choudhury, S. L. Chaplot.
  "Atomistic modeling of the vibrational and thermodynamic properties of uranium dioxide, UO<sub>2</sub>." J. Nucl.

- Mater. 377 (2008) 438–443. https://doi.org/10.1016/j. jnucmat.2008.03.020.
- [22.] Y. Yun, D. Legut, P. M.
  Oppeneer. "Phonon
  spectrum, thermal
  expansion and heat
  capacity of UO₂ from firstprinciples." J. Nucl. Mater.
  426 (2012) 109–114.
  https://doi.org/10.1016/j.
  jnucmat.2012.03.017.
- [23.] J. K. Fink. "Thermophysical properties of uranium dioxide." *J. Nucl. Mater.* 279 (2000) 1–18. https://doi.org/10.1016/S0022-3115(99)00273-1.
- [24.] B. T. Wang, J. J. Zheng, X. Qu, W. D. Li, P. Zhang. "Thermal conductivity of UO<sub>2</sub> and PuO<sub>2</sub> from first-principles." *J. Alloys Compd.* 628 (2015) 267–271. https://doi.org/10.1016/j. jallcom.2014.12.204.
- [25.] W. D. Kingery, J. Francl, R. L. Coble, T. Vasilos. "Thermal Conductivity: X, Data for Several Pure Oxide Materials Corrected to Zero Porosity." J. Am. Ceram. Soc. 37 (1954)

- 107–110. https://doi. org/10.1111/j.1551-2916.1954.tb20109.x.
- [26.] M. Sheindlin, D. Staicu, C. Ronchi, L. Game-Arnaud, B. Remy, A. Degiovanni. "Experimental determination of the thermal conductivity of liquid  $\mathrm{UO}_2$  near the melting point." J. Appl. Phys. 101 (2007). https://doi. org/10.1063/1.2721091.
- [27.] V. G. Baranov, Y. N. Devyatko, A. V. Tenishev, A. V. Khlunov, O. V. Khomyakov. "New method for determining the temperature dependence of the thermal conductivity coefficient of dielectrics in a pulse experiment." Inorg. Mater. Appl. Res. 1 (2010) 167–173. https://doi.org/10.1134/ S2075113310020164.
- [28.] R. L. Gibby. "The effect of plutonium content on the thermal conductivity of (U, Pu)O<sub>2</sub> solid solutions." *J. Nucl. Mater.* 38 (1971) 163–177. https://doi.org/10.1016/0022-3115(71)90040-7.

- [29.] J. L. Bates. *High-temperature Thermal Conductivity of "Round Robin" Uranium Dioxide*.
  BNWL-1431. Brookhaven National Laboratory. 1970.
- [30.] J. W. L. Pang, W. J. L. Buyers, A. Chernatynskiy, M. D. Lumsden, B. C. Larson, S. R. Phillpot. "Phonon lifetime investigation of anharmonicity and thermal conductivity of UO<sub>2</sub> by neutron scattering and theory." Phys. Rev. Lett. 110 (2013) 1–5. https://doi.org/10.1103/PhysRevLet.110.157401.
- [31.] H. Kim, M.H. Kim, M. Kaviany, Lattice thermal conductivity of UO₂ using ab-initio and classical molecular dynamics, J. Appl. Phys. 115 (2014). https://doi.org/10.1063/1.4869669.

Distributed Partnership at a Glance		
NSUF Institution	Facilities and Capabilities	
Argonne National Laboratory	The Intermediate Voltage Electron Microscopy  — Tandem Facility	
Collaborators		
Argonne National Laboratory	Memei Li (collaborator), Wei-Ying Chen (collaborator)	
Los Alamos National Laboratory	Aiping Chen (collaborator)	
Penn State University	Zefeng Yu (co-principal investigator)	
University of Florida	Ali Muntaha (collaborator), Michael Tonks (co-principal investigator)	

### SHORT COMMUNICATIONS

#### Ion Irradiation for High Fidelity Simulation of High Dose Neutron Irradiation

Todd Allen - University of Michigan - traumich@umich.edu



raditionally, research to understand radiationinduced changes in materials is conducted via radiation effects experiments in test reactors, followed by a comprehensive postirradiation characterization plan. Ion irradiations have been developed to the point where temperature is extremely well controlled and monitored, and damage rate and total damage are also measured continuously throughout the irradiation and with great accuracy. The objective of this project is to demonstrate the capability to predict the properties of structural materials in reactor and at high doses, using ion irradiation as a surrogate for reactor irradiations.

#### Experimental or Technical Approach

Dual ion irradiations were performed on T91 steel utilizing the dual beam configuration at the Michigan Ion Beam Laboratory using 5 MeV iron ions with a helium co-injection rate of about 4 appm He/dpa to a total damage of up to 35 dpa at temperatures of 406–570°C to complement irradiation of the same alloy in the BOR-60 reactor up to 35 dpa at temperatures from 360-525°C. Additional single beam ion irradiations were conducted on T91 to isolate the role of irradiation damage rate and co-injected helium. These experiments were used in conjunction with rate theory models of cavity evolution, helium portioning, and a more detailed cluster dynamics model.

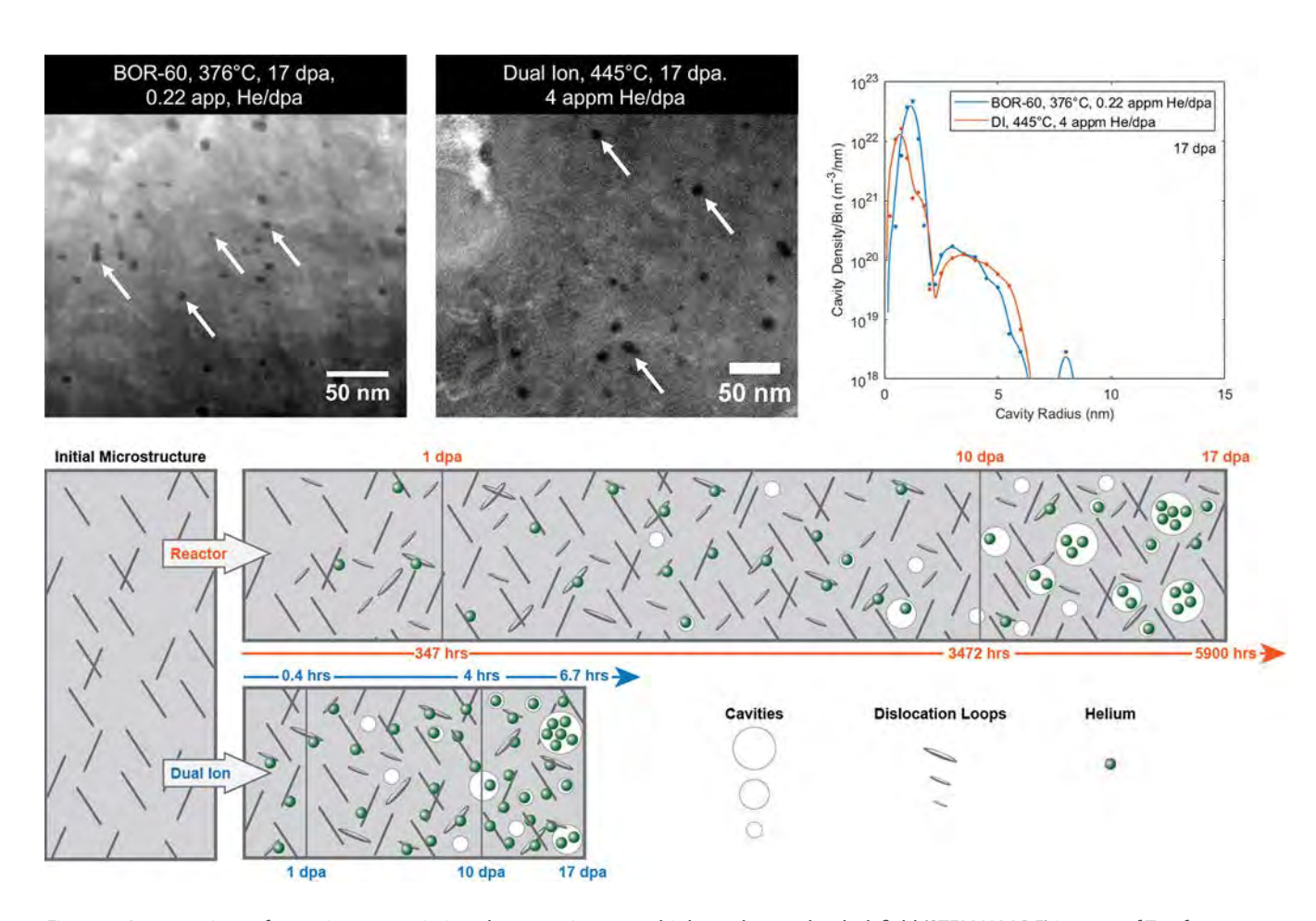


Figure 1. A comparison of scanning transmission electron microscopy high-angle annular dark field (STEM HAADF) images of T91 from BOR-60 irradiation and complementary dual ion irradiation with corresponding cavity size distributions (above) and schematic of the time-dependent helium trapping and release behavior under reactor and ion irradiation conditions (below).

#### **Results**

The microstructure from the dual ion irradiation was characterized using transmission electron microscopy (TEM) and compared with the BOR-60 irradiated steel. Cavities were characterized using high angle annular dark field scanning TEM. Additional characterization was performed to identify cavities smaller than 2 nm in radius using over focused and under focused bright field TEM imaging with a Gatan OneView 16-megapixel charge-coupled device (CCD) camera capable of 4K resolution with 0.25 nm point-to-point resolution. Hand counting techniques were used with the FIJI image software to measure the cavity diameter to convert to a cavity radius and estimate the density of cavities from resulting images. Images

for cavities can be found in the supplemental materials for Taller and Was' 2020 article [1]. Dislocation loops were imaged using on-zone STEM BF imaging near the [001] or [011] zone axis to view dislocation loops on edge, or nearly on edge, to distinguish between a < 100 > dislocation loops, a/2 < 111 > dislocationloops, and dislocation lines. The dislocation and cavity microstructures of dual ion irradiated T91 and T91 irradiated in the BOR-60 fast reactor matched extremely well using a temperature shift of +60-70°C and an increase in the helium injection ratio.

#### **Discussion/Conclusion**

Higher damage rates in ion irradiation require higher irradiation temperatures to maintain a balance

between defect production and loss: however, with helium transmutation, the temperature shift is less than predicted by invariance relationships. Higher rates of helium implantation are required in dual ion irradiations to compensate for the reduced irradiation time that impacts the distribution of helium among the microstructural features. The temperature dependence of swelling is governed by both the thermal evaporation of small vacancy clusters and helium trapping at damage rate independent trapping sites. These conclusions provide a guiding "formula" for predicting the complex radiation induced phenomenon of cavity nucleation and growth at an accelerated damage rate.

#### References

- [1.] S. Taller, and G. S. Was.
  "Understanding Bubble
  and Void Nucleation
  in Dual Ion Irradiated
  T91 Steel using Single
  Parameter Experiments."
  Acta Materialia. Vol.
  198. October 1, 2020.
  pp. 47–60, https://
  doi.org/10.1016/j.
  actamat.2020.07.060.
- [2.] Taller, S., and G. S. Was.
  "Understanding Bubble
  and Void Nucleation
  in Dual Ion Irradiated
  T91 Steel using Single
  Parameter Experiments."
  Acta Materialia. vol.
  198. October 1, 2020.
  pp. 47–60, https://
  doi.org/10.1016/j.
  actamat.2020.07.060.
- [3.] Taller, S., F. Naab, and G. S. Was. "A Methodology for Customizing Implantation Profiles of Light Ions Using a Single Thin Foil Energy Degrader." Nuclear Inst. and Methods in Physics Research:

  B. vol. 478. September
  1, 2020. pp. 274–283. https://doi.org/10.1016/j. nimb.2020.07.017.

#### **Publications**

[1.] Taller, S., G. VanCoevering, B. D. Wirth, and G. S. Was. "Predicting Structural Material Degradation in Advanced Nuclear Reactors with lon Irradiation." Scientific Reports, vol. 11. 2949. 2021, https://doi.org/10.1038/ s41598-021-82512-w.

Distributed Partnership at a Glance		
NSUF Institution	Facilities and Capabilities	
University of Michigan	Michigan Ion Beam Laboratory	
Collaborators		
University of Michigan	Stephen Taller (collaborator), Valentin Pauly (collaborator), Gabriella Bruno (collaborator), George Jiao (collaborator), Kevin Field (collaborator)	

# Bubble Formation of In situ He-Implanted 14YWT and CNA Advanced Nanostructured Ferritic Alloys

Yan-Ru Lin - University of Tennessee, Knoxville - ylin52@vols.utk.edu



he objective of this work is to investigate the effects of nanoparticle density and their binding energy on the formation of helium bubbles. The synergistic effect of helium along with radiation damage can cause unwanted degradation of the mechanical performance of structural materials and impact the safety of nuclear reactors [1]. It has been proposed that these effects could be mitigated by increasing the number of He trapping sites to control the bubble size or to shield the grain boundaries from He [2]. This concept has led to the development of nanostructured alloys with engineered high sink-strength microstructures.

# Experimental or Technical Approach

Helium bubble formation in Fe-9/10Cr binary alloys and two dispersion strengthened nanostructured alloys (CNA3 and 14YWT containing carbide and oxide particles, respectively) was examined by scanning/transmission electron microscopy (S/TEM) after ex situ and in situ He implantation to ~10,000 appm at 500–900°C. The thin TEM foils were irradiated at the Intermediate Voltage Electron Microscopy (IVEM)-Tandem facility in Argonne National Laboratory. The TEM thin foils of Fe-10Cr, CNA3, and 14YWT materials were irradiated with a 10 keV single He ion beam at a 15 degree incident angle, at 600 and 900°C. For the 600°C in situ irradiated

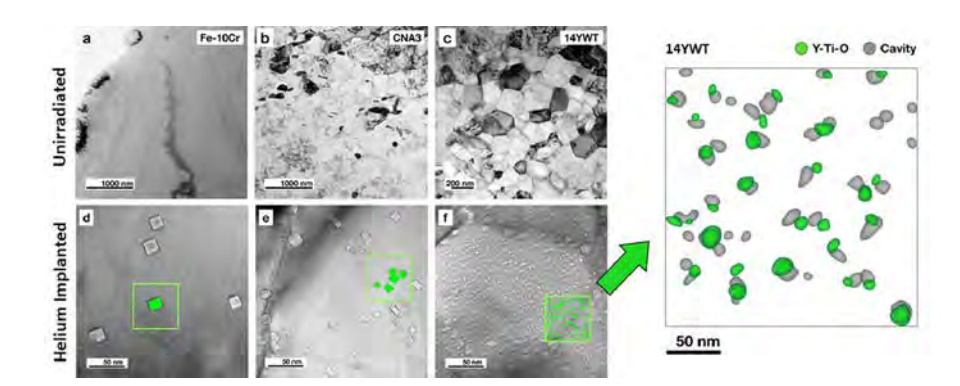


Figure 1. Under focused TEM images of bubbles in in situ He-implanted Fe-10Cr and NFA thin foils at  $600^{\circ}$ C (a–c) and  $900^{\circ}$ C (d-f). The green filled portions of the micrographs highlight the bubbles in the materials.

samples, once we achieved the target dose, we stopped the implantation and performed post irradiation annealing to 900°C. The annealing results were used to compare with the 900°C directly hot implanted experiments.

In situ TEM combined with post irradiation analysis using high resolution scanning transmission electron

microscopy (STEM) and electron energy loss spectroscopy (EELS) techniques were utilized to examine the microstructures. TEM magnifications of 100 kx or 200 kx were used for measuring the bubble sizes. Analysis of the STEM-EELS data was performed using Gatan GMS software. The spatial distribution and morphologies of various types of nanoparticles were evaluated from elemental maps acquired by STEM-EELS.

#### **Results**

Cavity formation in bulk He irradiated and in situ He irradiated ferritic alloys containing different nanoparticle densities: Fe-9/10Cr (without nanoparticles), CNA3 (intermediate), and 14YWT (highest nanoparticle density) was examined from 500 to 900°C by TEM and STEM. At all temperatures, the cavity density in the He implanted materials was generally in the order of Fe-9/10Cr < CNA3 < 14YWT, which directly corresponds to the nanoparticle density, whereas the cavity size showed the opposite order. The observed bubble number densities for the nanostructured alloys are comparable to the nanoparticle density, suggesting that the nanoparticles in both alloys

were effective in trapping He. The combination of high resolution STEM images and EELS revealed that the MX carbides in CNA3 and Y-Ti-O oxides/TiN particles in 14YWT showed a good capability for trapping He bubbles. The Y-Ti-O nanoparticles in 14YWT were uniformly distributed and exhibited a one to one relationship for bubble attachment to the nanoclusters. In the *in situ* experiment at 900°C, grain boundary cracking was severe in the Fe-10Cr model alloy but not in the nanostructured alloys.

#### **Discussion/Conclusion**

In agreement with previous studies, the addition of high-density nanoparticles were found to sequester the helium into finely dispersed tiny

bubbles at the particle-matrix interface (leading to a lower volume swelling compared to conventional alloys) and suppress He diffusion to the grain boundaries. The present results suggest that very high He concentrations can be managed well in nanostructured alloys with a high density of nanoparticles (>10<sup>22</sup> m<sup>-3</sup>, which corresponds to a sink strength  $> 10^{15}$  m<sup>-2</sup>). Furthermore, nanoparticles in both the CNA3 and 14YWT allovs were found to exhibit high (favorable) binding energies for helium cavities up to temperatures as high as 900°C.

#### References

- [1.] Dai, Y., G. R. Odette, and T. Yamamoto. "The effects of helium in irradiated structural alloys." R.J.M. Konings (Ed.), Comprehensive Nuclear Materials, Elsevier, Oxford. 2012. pp. 141–193.
- [2.] Odette, G. R., M. J. Alinger, and B. D. Wirth. "Recent developments in irradiation-resistant steels." *Annu. Rev. Mater. Res.* Vol. 38 (1). 2008. pp. 471–503.

#### **Publications**

#### **Journal**

[1.] Lin, Y., W. Chen, L. Tan, D. T. Hoelzer, Z. Yan, C. Hsieh, C. Huang, and S. J. Zinkle. "Bubble formation in helium-implanted nanostructured ferritic alloys at elevated temperatures." Acta Materialia. Vol. 217. 2021. p. 117165.

#### Conference

[2.] Lin, Y., W. Chen, L. Tan, D. T. Hoelzer, Z. Yan, C. Hsieh, C. Huang, and S. J. Zinkle. "Bubble formation in helium-implanted nanostructured 14YWT and CNA ferritic alloys at elevated temperatures." The Nuclear Materials Conference (NuMat). 2018. Seattle, Washington. October 2018. (Poster).

Distributed Partnership at a Glance		
NSUF Institution	Facilities and Capabilities	
Argonne National Laboratory	The Intermediate Voltage Electron Microscopy  — Tandem Facility	
Collaborators		
University of Tennessee, Knoxville	Steven Zinkle (co-principle investigator), Wei-Ying Chen (collaborator), Lizhen Tan (collaborator), David Hoelzer (collaborator)	

#### Changes in Mechanical and Chemical-Structural Properties of Gamma Irradiated Calcium Silicate Hydrates to an Absorbed Dose of 200 MGy with Respect to Pristine Samples

Nishant Garg - University of Illinois - nishantg@illinois.edu



alcium silicate hydrates (C-S-H) subjected to gamma irradiation may suffer dehydration due to hydrolysis. This can cause a decrease in the viscous properties of the material decreasing its creep response. In this proposal, the potential drop of viscous and elastic responses of C-S-H after a gamma dose (200 MGy) relevant to extended operation of light water reactors to 80 years was tested for the first time. Stress relaxation, creep, and Young's modulus were examined with nanoindentation. Responses from irradiated and control samples were compared. Morphological and chemical-structural properties were also be measured with X-ray power diffraction (XRD), Thermogravimetric Analysis (TGA), and transmission electron microscopy (TEM).

## Experimental or Technical Approach

Three loading scenarios were studied using a nano-indenter: (1) constant load for 2 minutes to derive the creep compliance, (2) constant indentation depth for 2 minutes to obtain the stress relaxation curves, and (3) constant load for 10 seconds to calculate the Young's modulus allowing the derivation of the viscoelastic and elastic properties of the irradiated and control samples. TEM bright field images of the control and the irradiated samples were taken, as well as some chemical point analysis with EDS to compare composition and morphology before and after irradiation for both types of samples. XRD patterns of irradiated and control samples were taken to compare structure parameters, such as the basal spacing and any other structural change (decomposition/ crystallization of other phases). TGA was used to study changes in water content.

#### **Results**

Creep compliance and stress relaxation were measured 100 times in each sample, while the Young's modulus was derived by 200 indents. In all cases erroneous indents were discarded and a statistical analysis was performed with bootstrap methods to obtain a mean. While no trends in viscous behavior (creep and relaxation) were clearly observed, an increase of Young's modulus was found for all irradiated samples with respect to their control specimens. XRD revealed a decrease in basal spacing (shift of the low angle reflection to higher angles). This matched findings by TGA that indicated a decrease in chemically bound water (0-400°C). Both XRD and TGA confirmed the loss of interlayer water due to hydrolysis. The increase in Young's modulus, or stiffening of the samples, was attributed to a densification due to water loss in the interlayer. TGA also revealed an increase in

water associated to hydroxyl groups (400–1000°C), which was later confirmed by complementary <sup>1</sup>H and <sup>29</sup>Si nuclear magnetic resonance experiments at Univerity of Illinois-Urbana Champain, The Nuclear Magnetic Resonance Spectroscopy (NMR) studies suggested Si-OH bond formation to gamma ray exposure.

#### **Discussion/Conclusion**

The findings of this research are important to understand and predict the impact of irradiation on concrete structures that are exposed to in service life doses in light water reactors. Neutron irradiation induced stresses in concrete can be dissipated by cracking or by relaxation of the cement paste. Calcium silicate hydrates are the main phase in hydrated cement. They lose water from hydrolysis after exposure to gamma rays, which increases their stiffness. This could affect the ability of the paste to relax stresses.

#### References

- [1.] Le Pape, Y., K. G. Field, and I. Remec. "Radiation effects in concrete for nuclear power plants, Part II: Perspective from micromechanical modeling." Nuclear Engineering and Design. vol. 282. 2015. pp. 144–157.
- [2.] Giorla, A., M. Vaitová, Y. Le Pape, and P. Štemberk. "Meso-scale modeling of irradiated concrete in test reactor." *Nuclear Engineering and Design*. vol. 295. 2015. pp. 59–73.
- [3.] Giorla, A. B., Y. Le Pape, and C. F. Dunant. "A creep-damage model for mesoscale simulations of concrete expansion-degradation phenomena." *CONCREEP-10.* 2015. pp. 537–540.
- [4.] Giorla, A. B., Y. Le Pape, and C. F. Dunant. "Computing creepdamage interactions in irradiated concrete."

- Journal of Nanomechanics and Micromechanics. vol. 7. 2017. p. 04017001.
- [5.] Tajuelo Rodriguez, E., W. A. Hunnicutt, P. Mondal, and Y. Le Pape. "Assessing the effects of gamma irradiation in concrete." Transactions of the American Nuclear Society Philadelphia. 2018. pp. 1649–1650.
- [6.] Tajuelo Rodriguez, E., W. A. Hunnicutt, Y. Le Pape, and P. Mondal. "Examination of gamma-irradiated C-S-H. Part I: Chemical-structural properties." *American Ceramic Society.* 2019. vol. 103. pp. 558–568 https://doi.org/10.1111/jace.16515.
- [7.] Hunnicutt, W. A., E.
  Tajuelo Rodriguez,
  P. Mondal, and Y. Le
  Pape. "Examination
  of Gamma-Irradiated
  Calcium Silicate Hydrates
  Part II: Mechanical
  Properties." Journal

of Advanced Concrete
Technology. vol.18, 2020.
pp. 558–570, doi:10.3151/
jact.18.558. This paper
was included in a Special
Issue of the Journal
of Advanced Concrete
Technology, entitled:
"Aging Management of
Concrete Structures in
Nuclear Power Plants
(Part II),"The special issue
was published/released,
on August 19, 2021.

#### **Publications**

#### **Presentations**

[1.] Tajuelo Rodriguez, E., and W. A. Hunnicutt, "Effects of Gamma Irradiation on C-S-H." Workshop on Effects of Gamma Irradiation of Cement Systems, International Committee of Irradiated Concrete. November 20, 2020.Conference

#### **Posters**

[2.] Tajuelo Rodriguez, E., A. Baral, W. A. Hunnicutt, N. Garg, and Y. Le Pape, "Effects of gamma irradiation on C-S-H structure and mechanical properties." Advanced Materials for Sustainable Infrastructure Development, Cutting-Edge Developments and Characterization of Cement-Based Materials, Gordon Research Conference. February 23-28, 2020. Ventura California.

#### **Journals**

[3.] Baral, A., E. Tajuelo
Rodriguez, W. A.
Hunnicutt, Y. Le Pape, T.
M. Rosseel, and N. Garg,
"Ultra-High Gamma
Irradiation of Calcium
Silicate Hydrates:
Evidence of Damage
in <sup>1</sup>H and <sup>29</sup>Si Atomic
Environments." submitted
and under review.

Distributed Partnership at a Glance		
NSUF Institution	Facilities and Capabilities	
Oak Ridge National Laboratory	Low Activation Materials Design and Analysis Laboratory	
Collaborators		
Oak Ridge National Laboratory	Elena Tajuelo Rodriguez (co-principal investigator), Yann Le Pape (collaborator)	
University of Illinois, Urbana- Champaign	Aniruddha Baral (collaborator)	

### In Situ SEM Irradiation Enhanced Creep Studies of 14 YWT

David Frazer - Idaho National Laboratory - david.frazer@inl.gov



he goal of this project is to evaluate the effects of irradiation on the creep properties of 14 YWT using the I<sup>3</sup>TEM at Sandia National Laboratory, which allows simultaneous mechanical testing during ion beam irradiation at elevated temperatures.

# Experimental or Technical Approach

A sample of 14 YWT was mechanical polished to 50 um thick. A focused ion beam instrument was then used to mill away excess material until 10s of nanopillars were produced. The dimensions of the nanopillars were 280 nm thick × 280 nm wide  $\times$  650–700 nm in height and were spaced 5 µm apart. The *in situ* TEM experiments were performed on the I<sup>3</sup>TEM at Sandia National Laboratory. This allows imaging of the sample while being irradiated with ions. In addition, the Hysitron

PI-95 pico-indenter enables instrumented indentation in the TEM for mechanical testing. Room temperature compressive creep experiments were performed under 2.8 MeV Au<sup>4+</sup> ion beam irradiation and with no irradiation. With thickness of the pillars at 25 degrees and 2.8 MeV Au<sup>4+</sup> ions, the peak displacement damage rate in the material is calculated to be 0.028 dpa/s using the SRIM code employing the standard composition of 14 YWT and a displacement energy of 40 eV. (The pillar is orientated at a 25 degree angle rather than being perpendicular to the beam.) For the compression creep experiments, the PI-95 was used in load control mode. The pillars were loaded to approximately 450 MPa (50 µN load) and held for 300 seconds to measure the change in displacement with time. For these experiments, three nanopillars were tested under each condition.

#### **Results**

The strain rate was found to increase under irradiation going from negligible levels to  $6 \times 10^{-4}$  s<sup>-1</sup>. While this increase is higher than typical creep rates of 14 YWT, there are some experimental challenges with regard to sample geometry and size, dose rate, and other potential contributing factors. The capability to see a difference in the creep strain rate between the two conditions shows promise for in situ experiments for the I<sup>3</sup>TEM and the I<sup>3</sup>SEM. There are some challenges with sample preparation and use of the TEM with magnetic samples that would make elevated temperature experiments more difficult. The stability of the nanoindenter system could allow for more sophisticated experiments. In the future the damage rate from the beam or strain rate jump tests could be performed to

gather more information from an experiment on a single pillar. This would allow for the rapid evaluation of the creep properties of different materials in the future.

#### **Discussion/Conclusion**

This project demonstrated the ability to see a difference in microscale creep properties between irradiated and nonirradiated material samples It suggests there is the possibility for elevated temperature experiments and for similar studies on large specimens in the I<sup>3</sup>SEM at Sandia National Laboratory. While there were some technical challenges associated with sample shape and geometry in the I3TEM, experiments using of larger specimens in the I<sup>3</sup>SEM will

allow the measurement of macroscale creep properties. This could allow for the rapid evaluation of materials properties in ion beam irradiation environments.

#### **Publications**

[1.] R. J. Parrish, D. C. Bufford, D. M. Frazer, C. A. Taylor, J. Gutierrez-Kolar, D. L. Buller, B. L. Boyce, and K. Hattar. "Exploring Coupled Extreme Environments via In-situ Transmission Electron Microscopy." Microscopy Today, Vol. 29. 1. 2021. pp. 28–34. doi:10.1017/S1551929520001595.

Distributed Partnership at a Glance		
NSUF Institution	Facilities and Capabilities	
Sandia National Laboratory	oratory SNL Ion Beam Laboratory	
Collaborators		
Los Alamos National Laboratory	Tarik Saleh (co-principal investigator), Stuart Maloy (co-principal investigator), Joshua White (co-principal investigator)	

### Ion Irradiation of ThO<sub>2</sub> and UO<sub>2</sub> Single Crystals

Marat Khafizov - Ohio State University - khafizov. 1@osu.edu

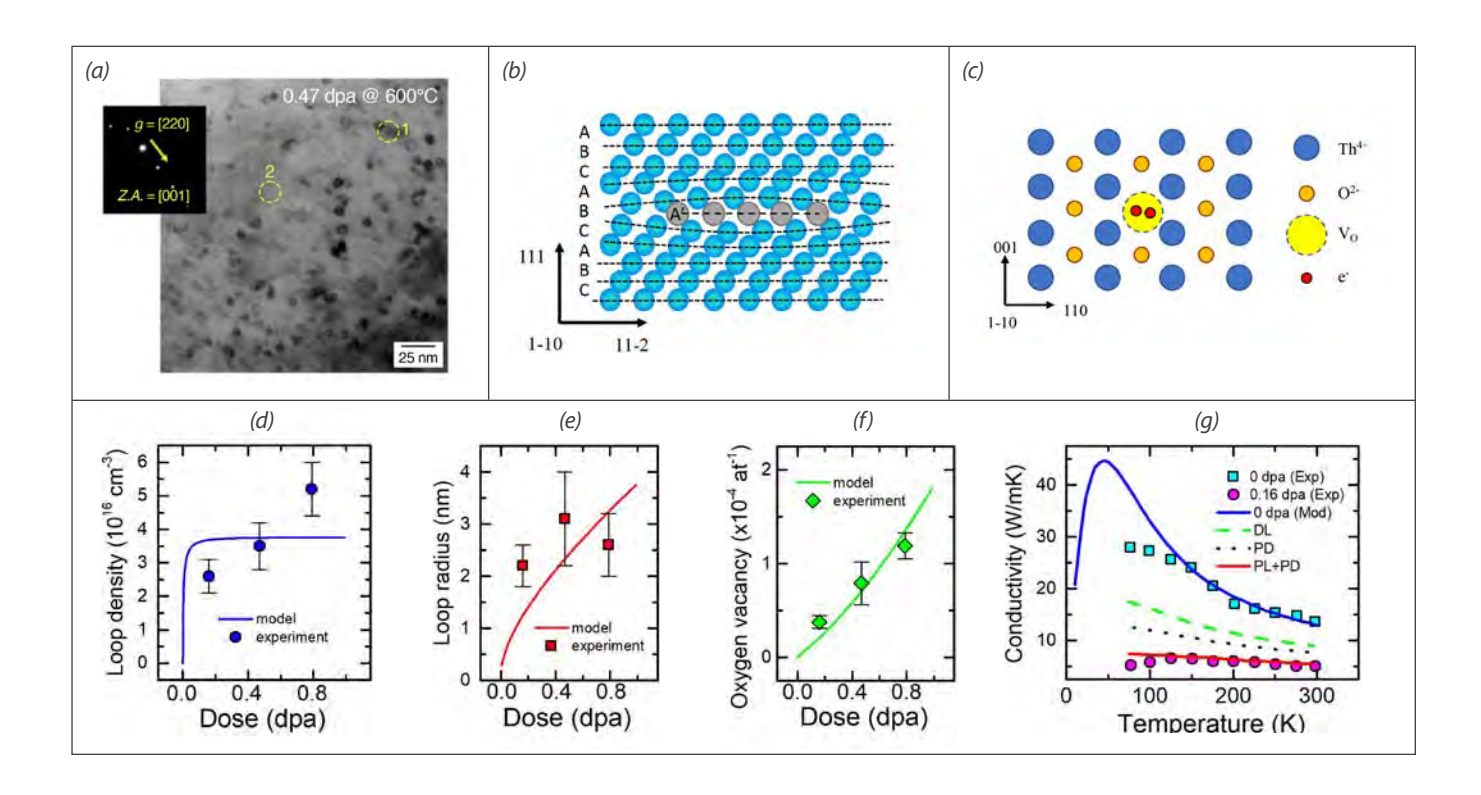


he goal of this project was to investigate the impact of irradiation induced defects on thermal transport in nuclear fuel materials. Considering previous irradiation of CeO<sub>2</sub> and UO<sub>2</sub> using light ions, two irradiation temperature regimes were considered [1,2]. The first room temperature regime targeted a microstructure dominated by point defects. The second irradiation, performed at 600°C, targeted a microstructure dominated by interstitial dislocation loops. Two MeV protons were selected to develop a uniform damage profile into the top 20 µm of the sample for spatially resolved thermal conductivity measurement [3].

# Experimental or Technical Approach

Single crystals of ThO<sub>2</sub> and UO<sub>2</sub> obtained using the hydrothermal growth approach were provided by the Air Force Research Laboratory. Irradiations were performed utilizing the ion beam accelerator at Texas A&M University using 2 MeV protons up to estimate doses of 0.2 and 0.8 dpa at room temperature

and at 600°C, respectively. Extensive characterization has been performed on the irradiated single crystal thoria sample. Transmission electron microscopy (TEM) characterization of extended defects induced by ion irradiation was performed using facilities located at Idaho National Laboratory's Irradiated Materials Characterization Laboratory (IMCL) and included FEI Ouanta 3D FEG Dual Beam focused ion beam for TEM lamellae preparation and Thermo Scientific Titan Themis TEM. Subsequently, additional microstructure characterization of point defects was conducted using Raman spectroscopy, photoluminescence spectroscopy, and optical spectroscopic ellipsometry. The impact of defects on thermal conductivity was measured using a modulated thermoreflectance approach [4]. Microstructure evolution was analyzed using rate theory modeling [5,6]. Thermal conductivity was analyzed using both classical models for thermal transport [1,2] with input from first principles calculations [9,10].



#### **Results**

Bright field image combined with rel-rod dark field TEM image analysis was used to observe and quantify the diameter and density of dislocation loops in the high-temperature irradiated samples [7]. Using standard  $\overrightarrow{g} \cdot \overrightarrow{b}$  analysis and inside-outside contrast methods, the loops were determined to be 1/3(111){111} oriented interstitial Frank faulted loops [8]. Characterization performed using Raman and

optical spectroscopies revealed an abundance of point defects and small defect clusters in both room- and high-temperature irradiated samples. These observations suggested that at 600°C some of the point defects are not sufficiently mobile to ensure their recombination or absorption by extended defects [7]. This is in contrast to the loop dominated microstructure observed in polycrystalline ceria irradiated at 700°C [1]. The abundance of point

Figure 1. Characterization of proton irradiated single crystal  $ThO_2$ . (a) Bright field TEM image revealing dislocation loops [8]. (b) 1/3(111){111} loop structure revealed by  $\overrightarrow{g} \cdot \overrightarrow{b}$  invisibility criterion analysis [8]. (c) The proposed structure of oxygen vacancy visible in optical spectroscopy. Evolution of (d) dislocation loop density, (e) loop diameter, and (f) oxygen vacancy concentration obtained from experimental characterization [10]. Solid lines are result of rate model predictions parametrized using these results. (g) Thermal conductivity reduction analysis [10].

defects in thoria is consistent with the rate theory modeling analysis of microstructure [10]. Thermal conductivity analysis revealed that the conductivity reduction as a function of dose is due to point defects in room temperature irradiated samples as expected. However, for the high temperature irradiated samples, the conductivity is limited by phonon scattering by extended defects as well as by point defects on thorium sublattice.

## **Discussion/Conclusion**

lon irradiation and extended defect characterization enabled by this NSUF project revealed information on microstructure evolution in ThO<sub>2</sub> under irradiation. The experimental data is critical to furthering our fundamental understanding of the behavior of irradiated nuclear fuels.

#### References

- [1.] Khafizov, M., J. Pakarinen, L. He, and D. H. Hurley. "Impact of irradiationinduced dislocation loops on thermal conductivity in ceramics." J. Amer. Ceram. Soc. vol. 102. 2019. 7533.
- [2.] Khafizov, M., M. F. Riyad, Y. Wang, J. Pakarinen, L. He, T. Yao, A. El-Azab, D. H. Hurley. "Combining mesoscale thermal transport and x-ray diffraction measurements to characterize early-stage evolution of irradiation-induced defects in ceramics." Acta Materialia. vol. 193. 2020. pp. 61–70.
- [3.] Riyad, F., V. Chauhan, and M. Khafizov.

  "Implementation of a multilayer model for measurement of thermal conductivity in ion beam irradiated samples using a modulated thermoreflectance approach."

  J. Nucl. Mater. vol. 509. 134 (2018).
- [4.] D. H. Hurley, R. S. Schley, M. Khafizov, B. L. Wendt. "Local measurement of

- thermal conductivity and diffusivity." *Rev. Sci. Instrum.* vol. 86. 2015. 123901.
- [5.] V. S. Chauhan, J. Pakarinen, T. Yao, L. He, D. Hurley and M. Khafizov. "Indirect Characterization of Point Defects in Proton Irradiated Ceria." *Materialia*. vol. 15. 2021. 101019.
- [6.] L. He, M. Khafizov, C. Jiang, B. Tyburska-Püschel, B. Jaques, P. Xu, M. Meyer, K. Sridharan, D. P. Butt, J. Gan. "Phase and defect evolution in uranium-nitorgen-oxygen system under irradiation." Acta Materialia. vol. 208. 2021. 116778.
- [7.] C. A. Dennett, Z. Hua,
  A. Khanolkar, T. Yao, P. K.
  Morgan, T. A. Prusnick,
  N. Poudel, A. French, K.
  Gofryk, L. He, L. Shao,
  M. Khafizov, D. B. Turner,
  J. M. Mann, and D. H.
  Hurley. "The influence
  of lattice defects and
  recombination on thermal
  transport in single crystal
  thorium dioxide." APL
  Materials. vol. 8. 2020.
  111103.

- [8.] K. Bawane, X. Liu, T. Yao, Marat Khafizov, A. French, J. M. Mann, L. Shao, J. Gan, D. H. Hurley, L. He. "TEM Characterization of Dislocation Loops in Proton Irradiated Single Crystal ThO<sub>2</sub>." Journal of Nuclear Materials. vol. 55. 2021. 152998.
- [9.] W. R. Deskins, A. Hamed, T. Kumagai, C. A. Dennett, J. Peng, M. Khafizov, D. Hurley, A. El-Azab. "Thermal conductivity of ThO₂: Effect of point defect disorder." J. Appl. Phys. vol. 129. 2021. 075102.
- [10.] C. A. Dennett, W. R. Deskins, Marat Khafizov, Z. Hua, A. Khanolkar, K. Bawane, L. Fu, J. M. Mann, C. A. Marianetti, L. He, D. H. Hurley, A. El-Azab. "An integrated experimental and computational investigation of defect and microstructural effects on thermal transport in thorium dioxide." Acta Materialia. vol. 213, 2021, 116934.

#### **Publications**

- [1.] C. A. Dennett, W. R. Deskins, Marat Khafizov, Z. Hua, A. Khanolkar, K. Bawane, L. Fu, J. M. Mann, C. A. Marianetti, L. He, D. H. Hurley, A. El-Azab. "An integrated experimental and computational investigation of defect and microstructural effects on thermal transport in thorium dioxide." Acta Materialia. vol. 213, 2021, 116934.
- [2.] K. Bawane, X. Liu, T. Yao, Marat Khafizov, A. French, J. M. Mann, L. Shao, J. Gan, D. H. Hurley, L. He. "TEM Characterization of Dislocation Loops in Proton Irradiated Single Crystal ThO<sub>2</sub>." Journal of Nuclear Materials. vol. 55. 2021. 152998.
- [3.] C. A. Dennett, Z. Hua, A. Khanolkar, T. Yao, P. K. Morgan, T. A. Prusnick, N. Poudel, A. French, K. Gofryk, L. He, L. Shao, M. Khafizov, D. B. Turner, J. M. Mann, and D. H. Hurley. "The influence of lattice defects and recombination on thermal transport in single crystal thorium dioxide." APL Materials. vol. 8. 2020. 111103.

Distributed Partnership at a Glance		
NSUF Institution	Facilities and Capabilities	
Idaho National Laboratory	Irradiated Materials Characterization Laboratory	
Collaborators		
Idaho National Laboratory	Lingfeng He (co-principal investigator), David Hurley (co-principal investigator)	

## Defect Clustering in 316H Stainless Steel and High Entropy Alloy Under In-situ Irradiation at 600-700°C

Wei-Ying Chen - Argonne National Laboratory - wychen@anl.gov

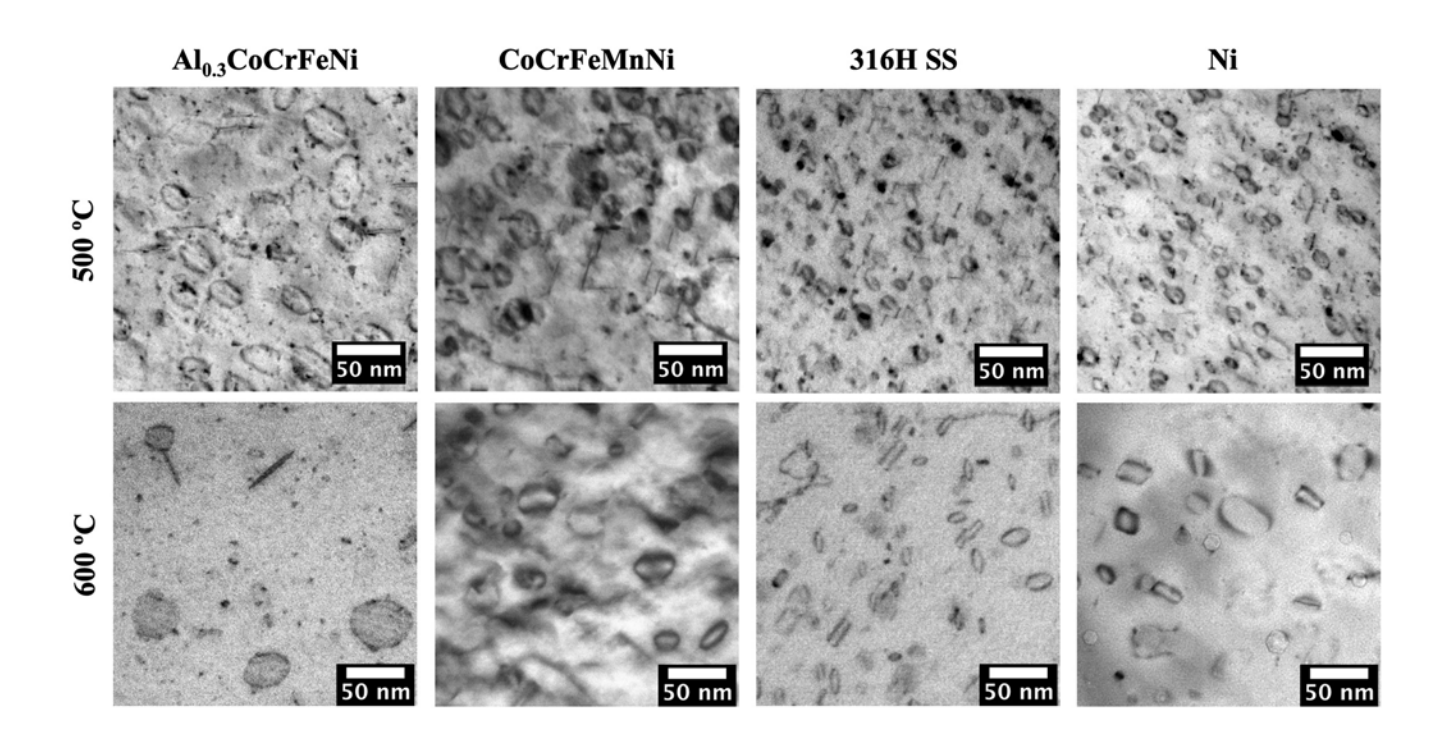


he objective of this study was to understand the irradiation behavior of high entropy alloys (HEAs) at elevated temperatures and to compare the irradiated microstructures between HEAs and 316H stainless steel (SS) and pure nickel. Under irradiation, several dynamic processes, such as cascade condensation. cluster dissociation, and loop unfaulting take place inside materials. A detailed understanding of each individual process and the interactions among them is necessary for unveiling the distinctive microstructure at high doses. This project was an initial attempt to lay down the groundwork for future effort on long term damage modeling and neutron irradiation experiments.

## Experimental or Technical Approach

Three millimeter transmission electron microscopy (TEM) specimens of Al<sub>0.3</sub>CoCrFeNi,

CoCrFeMnNi, 316H SS, and nickel were prepared and irradiated with 1 MeV krypton ions inside a Hitachi 9000 TEM operated at 300 kV. The irradiation experiments were carried out at 300°C, 500°C, 600°C, and 700°C, with a flux of  $6.3 \times 10^{11}$  ions/cm<sup>2</sup>/s or  $1.3 \times 10^{12} \text{ ions/cm}^2/\text{s}$ , reaching a final fluence of 6.3  $\times 10^{14}$  ions/cm<sup>2</sup> (1 dpa). The microstructures of the samples were observed in situ during irradiation under bright field (BF) and weak beam dark field imaging conditions. The irradiation induced dislocations, dislocation loops, and stacking fault tetrahedral (SFT) were imaged with a two beam imaging condition of g = 200 near 011 zone axis. The irradiation induced voids were imaged with an underfocused amount of 1 µm. The microstructural evolution was recorded for selected experiments with a range of video frame rates from 1 fps to 100 fps. Nanoindentation tests were also performed



on the specimens to provide complementary hardening information on irradiated materials.

## **Results**

The irradiation induced dislocation loops, SFT, and voids in Al<sub>0.3</sub>CoCrFeNi, CoCrFeMnNi, 316H SS, and nickel were observed and

analyzed as a function of irradiation dose and temperature. For the experiments at 500°C and above, a high density of SFT and a depletion of dislocation loops were visible in thin areas near the foil surface for all materials. In the thick regions of the specimens, dislocation loops were observed. A

Figure 1. BF TEM micrographs showing the dislocation loops in Al<sub>0.3</sub>CoCrFeNi, CoCrFeMnNi, 316H SS and nickel irradiated at 500°C and 600°C to 1 dpa.

through thickness analysis was performed to quantitatively evaluate the effect of foil surface on the observed defects for all samples.

For the materials and irradiation conditions studied in this work, void swelling was only observed in the nickel sample irradiated at 600°C. No voids can be seen under all other conditions and in the HEAs and 316H SS samples. The loop density and size were similar for the HEAs and 316H SS irradiated at 300°C [1]. At 500°C and 600°C, the loop density was much smaller and the size much larger, in the HEAs as compared with the 316H SS, as shown in Figure 1. This observation was consistent with the nanoindentation measurement where the 316H SS exhibited higher post irradiation hardening than the HEAs at 500°C [2].

## **Discussion/Conclusion**

The irradiated microstructures of HEAs, 316H SS, and pure nickel have been compared over a temperature range between 300°C and 700°C. The fundamental effect of the alloying complexity on the irradiation damage process has been revealed. The comparison of the irradiated microstructures of HEAs and 316H SS provides useful information for the potential applications of HEAs in nuclear reactor systems.

## References

[1.] Chen, W-Y., et al.

"Irradiation effects in high entropy alloys and 316H stainless steel at 300°C." Journal of Nuclear Materials. Vol. 510. 2018. pp. 421–430.

[2.] Chen, W-Y., et al. "Irradiation effects on Al<sub>0.3</sub>CoCrFeNi and CoCrMnFeNi highentropy alloys, and 316H stainless steel at 500°C."

Journal of Nuclear Materials.
Vol. 539, 2020, 152324.

## **Publications**

- [1.] Hashimoto, N., et al.

  "Effect of stacking fault
  energy on damage
  microstructure in ionirradiated CoCrFeNiMnx
  concentrated solid
  solution alloys." Journal of
  Nuclear Materials. vol. 545.
  2021. 152642.
- [2.] Chen, W-Y., et al.

  "Irradiation-induced
  segregation at
  dislocation loops in
  CoCrFeMnNi high
  entropy alloy." *Materialia*.
  vol. 14. 2020. 100951.

- [3.] Chen, W-Y., et al.,

  "Irradiation effects
  on Al<sub>0.3</sub>CoCrFeNi and
  CoCrMnFeNi high-entropy
  alloys, and 316H stainless
  steel at 500°C." Journal of
  Nuclear Materials. vol. 539.
  2020. 152324.
- [4.] Chen, W-Y., et al. "In-situ Observation of Irradiation Effects on High Entropy Alloys, 316H Stainless Steelsand Nickelat 500-

700°C." MiNES Conference. Baltimore, Maryland. October 6–10, 2019.

Distributed Partnership at a Glance		
NSUF Institution	Facilities and Capabilities	
Argonne National Laboratory	The Intermediate Voltage Electron Microscopy  — Tandem Facility	
Collaborators		
Argonne National Laboratory	Yiren Chen (co-principal investigator), Krishnamurti Natesan (co-principal investigator)	

## Atom Probe Characterization of Neutron Irradiated Commercial ZIRLO® and AXIOM X2® Alloys

Mukesh Bachhav - Idaho National Laboratory - mukesh.bachhav@inl.gov

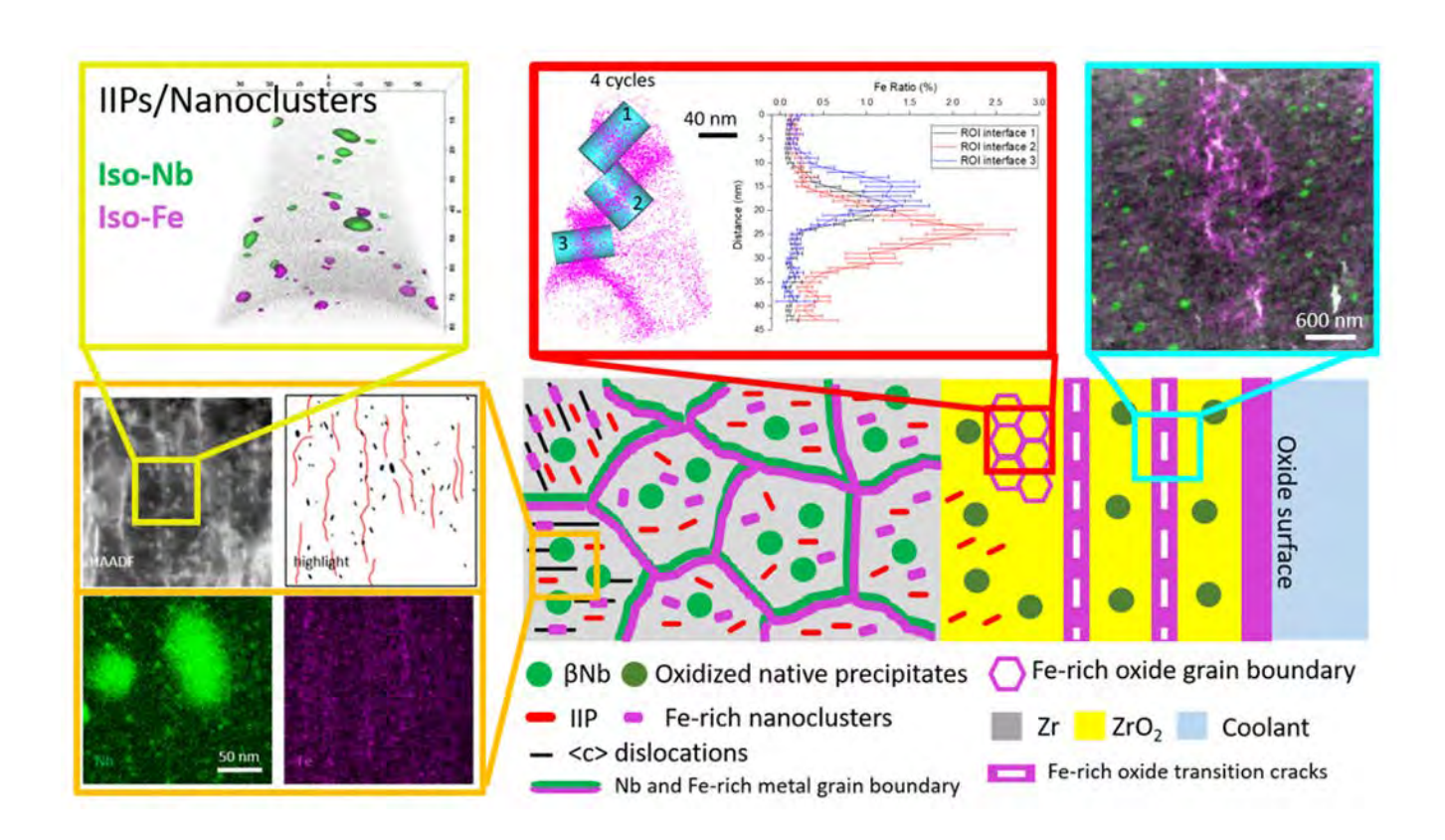


he hypothesis validated in this study is then reduced in reactor corrosion kinetics of Zr-Nb alloys, compared to other Zr-based fuel clad alloys is due to the irradiation induced reduction of Nb content in the Zr solid solution by the precipitation of Nb rich irradiation induced platelets (IIPs)/nanoclusters. The measurement of Nb concentration in the metal solid and oxide layer is key in understanding precipitation behavior and its role on corrosion kinetics. Although the instantaneous oxide/ metal velocity is relatively fast, the diffusion of Nb atoms is likely faster for Nb to reach an equilibrium state in the oxide by rejecting Nb atoms back into the metal matrix.

## Experimental or Technical Approach

Advanced commercial Zirconium-Niobium (Zr-Nb) alloys, such as ZIRLO® and AXIOM®, have been developed by Westinghouse

to enhance the corrosion resistance of fuel cladding material for longer service time. This study specifically aims at investigating the neutron irradiation induced Nb redistribution in AXIOM® X2® to understand the effect of neutron irradiation induced microchemistry changes and the irradiationenhanced corrosion resistance observed in Zr-Nb alloys. The uniqueness of these sets of neutron irradiated alloy samples is that they are at the same two extremes of the fuel cycles, allowing the microchemistry evolution to be studied as a function of irradiation doses, exposure time, and Sn content. To study the neutron IIP/nanoclusters and Nb concentration in the solid solution, atom probe tomography (APT) is the primary tool to obtain reliable chemical information. Sample preparation for the APT study was performed using the shielded focused ion beam at the Irradiated Materials



Characterization Laboratory (IMCL) at Idaho National Laboratory. This was followed by APT analysis in the MaCS at the Center for Advanced Energy Studies (CAES) facility to elucidate microstructural and chemistry changes in all samples.

#### **Results**

 The evolution of precipitates in the metal matrix of in pile X2® do not show much irradiated difference compared to other neutron irradiated recrystallized Zr-Nb alloys, such as M5®. Both Nb rich native precipitates and IIPs

Figure 1. Graphical abstract on microstructural and microchemistry changes in neutron irradiated X2 alloy using Atom Probe Tomography and Transmission Electron Microscopy along with schematic of overall microstructure in the oxide and matrix region.

were found in the metal matrix. Their composition tends to reach an equilibrium state of about 40 at.% Nb. The Nb rich IIPs/nanoclusters density and sizes in X2® follow the same trend reported in literature. There is no evidence showing Nb segregation to <c> dislocation loops, whereas Fe rich nanoclusters may decorate the <c> dislocation loops.

2. In the oxide, the Nb rich nanoclusters are likely to only exist at regions close to an oxide/metal (O/M) interface as observed by APT analysis. However, their oxidation state is still uncertain. At further distance from an O/M interface, the Nb rich nanoclusters may have fully dissolved. While Fe rich nanoclusters were not found in the oxide, Fe rich transition cracks and Fe rich oxide grain boundaries were observed. Those Fe rich features may be due to (1) trapping of coolant water with dissolved Fe or (2) segregation of Fe from supersaturated oxide solid solution. The second mechanism is supported by the nonequilibrium capture of Fe in the suboxide.

### **Discussion/Conclusion**

The major hypothesis validated in this study is the reduced in reactor corrosion kinetics of Zr-Nb alloys is due to the reduction of Nb content in the Zr solid solution by the precipitation of Nb rich IIPs/ nanoclusters. The Nb content in the oxide is even lower than in the metal matrix. The lower Nb content in the oxide solid solution led to a higher oxide space charge density, which induces a higher electric field across the oxide and lowers the corrosion rate.

#### References

- [1.] Doriot, S., et al.

  "Microstructural Stability
  of M5™ Alloy Irradiated
  up to High Neutron
  Fluences." Journal of ASTM
  International. vol. 2, no. 7,
  2005, pp. 1–24.
- [2.] Coleman, et al. "Precipitation in Zr--2.5 Wt.-% Nb During Neutron Irradiation." Phase Stability During Irradiation; Pittsburgh; Pa.; October 5-9 1980. 1980, pp. 587–599.
- [3.] Yu, Z., et al. "Irradiation-Induced Nb Redistribution of ZrNb Alloy: An APT Study." Journal of Nuclear Materials. vol. 516. 2019. pp. 100–110.
- [4.] Urbanic, V., et al. "Effect of Aging and Irradiation on the Corrosion of Zr-2.5 Wt. per Cent Nb." *Corrosion*. vol. 31, no. 1. 1975. pp. 15–20.

[5.] Motta, Arthur T., et al. "Corrosion of Zirconium Alloys Used for Nuclear Fuel Cladding." Annual Review of Materials Research. vol. 45. no. 1. 2015. pp. 311–343.

## **Publications**

[1.] Yu, Z., M. Bachhav, F. Teng, L. He, and A. Couet. "Nanoscale redistribution of alloying elements in high-burnup AXIOM-2 (X2®) and their effects on in-reactor corrosion." *Corrosion Science*. vol. 190. 2021. 109652.

Distributed Partnership at a Glance		
NSUF Institution	Facilities and Capabilities	
Center for Advanced Energy Studies	Microscopy and Characterization Suite	
Idaho National Laboratory	The Intermediate Voltage Electron Microscopy — Tandem Facility	
Collaborators		
University of Wisconsin	Zefeng Yu (collaborator), Adrien Couet (collaborator)	

# NSUF LIST OF ACRONYMS

AML	Activated Materials Laboratory
ANS	American Nuclear Society
APS	Advanced Photon Source
APT	Atom Probe Tomography
ATR	Advanced Test Reactor
BF	Bright Field
	Consolidated Innovative Nuclear Research
	Dark Field
DISECT	Disc Irradiation for Separate Effects Testing
dpa	displacements per atom
	Electron Energy Loss Spectrometry
EPMAD	Electron Microscope Pixel Array Detector
FaMUS	Fuels and Materials Understanding Scale
	Focused Ion Beam
HEA	High Entropy Alloys
	Irradiation Induced Platelets
IMCL	Irradiated Materials Characterization Laboratory
	Intermediate Voltage Electron Microscopy
	kilovolt
LAMDALow A	ctivation Materials Design and Analysis Laboratory
	Manual

ML	Machine Learning
MaCS	Microscopy and Characterization Suite
MiNES	Materials in Nuclear Energy Systems
MVP	MARMOT Validation Project
NEAMS	Nuclear Energy Advanced Modeling and Simulation
NFML	Nuclear Fuels and Materials Library
NMR	Nuclear Magnetic Resonance Spectroscopy
NSERT	. Nanostructured Steels for Enhanced Radiation Tolerance
NSLS-II	National Synchrotron Light Source II
NSUF	Nuclear Science User Facilities
PI	Principal Investigator
PIE	Post Irradiation Examination
	Rapid Turnaround Experiment
SAM-2	Sample-2
SFT	Stacking Fault Tetrahedral
	Sandia National Laboratories
SS	Stainless Steel
TEM	Transmission Electron Microscope
TGA	Thermo-Gravimetric Analysis
TRISO	TRI-structural ISOtropic
VDD	V Day Diffraction



## INDEX

## **NSUF & Partner Institutions:** Facilities & Capabilities:

Argonne National Laboratory (ANL): 14, 22, 34, 35, 38, 39, 45, 57, 62, 65, 76, 79

Argonne National Laboratory: *Advanced Photon Source (APS)*, 34, 84

Argonne National Laboratory: Activated Materials Laboratory (AML), 3, 34, 35, 84

Argonne National Laboratory: The Intermediate Voltage Electron Microscopy (IVEM) – Tandem Facility, 22, 34, 38, 39, 45, 46, 57, 62, 65, 79, 83, 84

Belgian Center for Nuclear Research (SCK/CEN): Belgian Reactor 2, Laboratory for High and Medium Activity, 11, 23

Brigham Young University: 15, 41

Brookhaven National Laboratory (BNL): 14, 57 Brookhaven National Laboratory: National Synchrotron Light Source II (NSLS-II), 16, 22, 84

Carnegie Mellon University: 15

Center for Advanced Energy Studies (CAES): 10, 14, 20, 21, 33, 36, 38

Center for Advanced Energy Studies: *Microscopy and Characterization Suite (MaCS)*, 20, 22, 38, 39, 40, 41, 81, 83, 84

General Electric Global Research: 15, 41

Idaho National Laboratory (INL): 2, 11, 14, 15, 24, 29, 30, 31, 36, 38, 39, 40, 41, 70, 75, 80

Idaho National Laboratory: Advanced Test Reactor (ATR), 16, 17, 18, 19, 37, 40, 84

Idaho National Laboratory: Analytical Laboratory (AL), 5

Idaho National Laboratory: High Performance Computing (HPC), 9

Idaho National Laboratory:

Irradiated Materials Characterization Laboratory (IMCL), 27, 30, 31, 42, 72, 75, 81, 84, 85

Idaho National Laboratory: *Materials & Fuels Complex* (MFC), 5, 30, 38, 39, 40, 41

Italian Institute of Technology: 15

Lawrence Livermore National Laboratory (LLNL): 14, 22

Los Alamos National Laboratory (LANL): 14, 22, 46, 57, 71

Massachusetts Institute of Technology (MIT): 14, 15, 22, 38, 39

Michigan Institute of Technology: 36

Nagoya University: 15, 39



North Carolina State University (NCSU): 14, 15, 22, 36

North Carolina State University: *Electric Power Research Institute*, 15, 39, 40

Oak Ridge National Laboratory (ORNL): 14, 15, 33, 41, 69

Oak Ridge National Laboratory: High Flux Isotope Reactor (HFIR), 22

Oak Ridge National Laboratory: Irradiated Materials Examination and Testing Facility (IMET) Hot Cells, 22 Oak Ridge National Laboratory: Low Activation Materials Design and Analysis Laboratory (LAMDA), 22, 39, 40, 41, 69, 84

The Ohio State University (OSU): 14, 72

The Ohio State University: The Ohio State University Nuclear Research Laboratory, 22

Oregon State University: 15, 38, 41

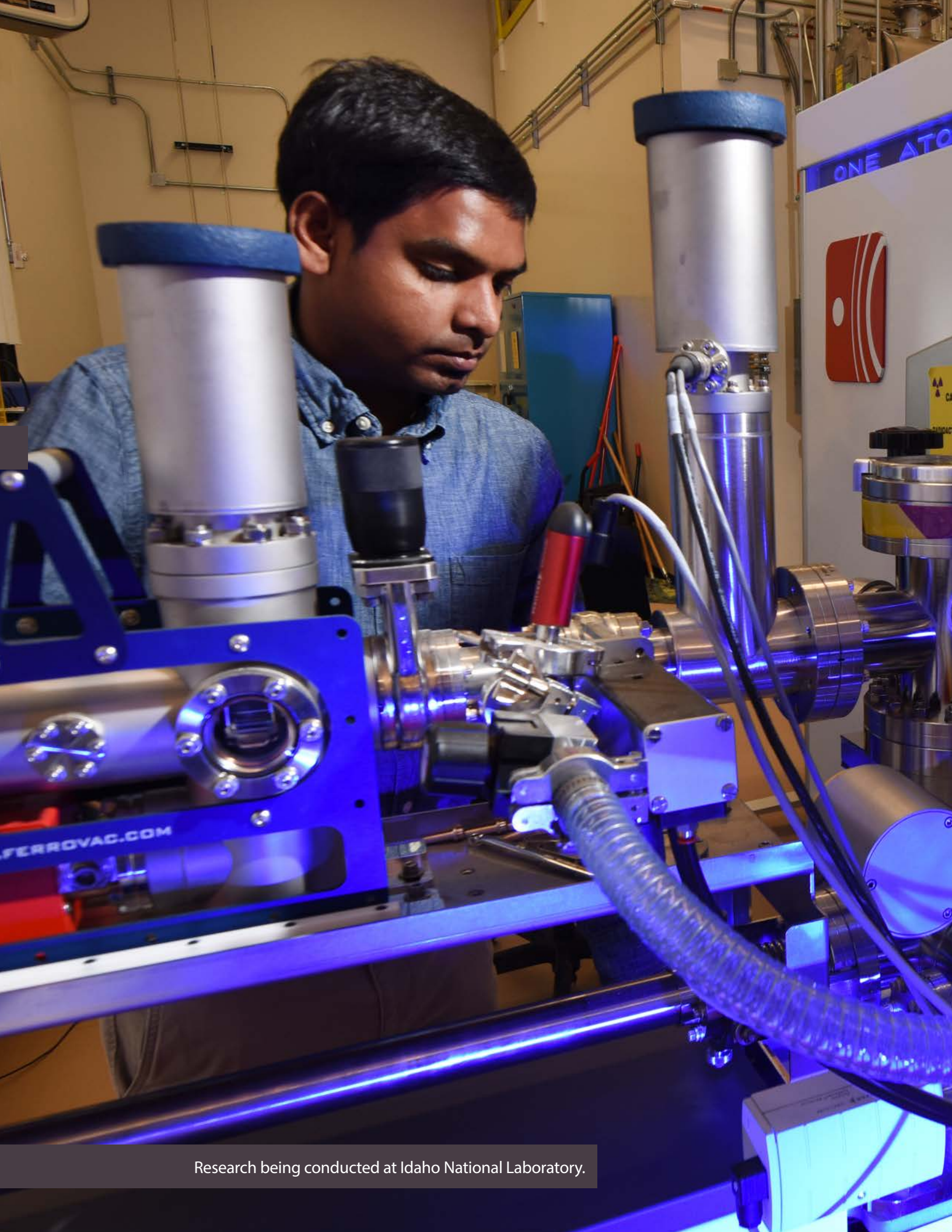
Pacific Northwest National Laboratory (PNNL): 14, 15 Pacific Northwest National Laboratory: *Materials Science & Technology Laboratory (MSTL)*, 22

Pacific Northwest National Laboratory: Radiochemical Processing Laboratory (RPL), 22

Penn State University: 44, 57

Purdue University: 14

Purdue University: Interaction of Materials with Particles and Components, 23



Purdue University: School of Materials Engineering, 32

Sandia National Laboratories (SNL): 14, 23, 84

Sandia National Laboratories: Annular Core Research Reactor, 23

Sandia National Laboratories: *SNL Ion Beam Laboratory*, 23, 71

Sandia National Laboratories: Sandia Pulse Reactor Facility Critical Experiment, 23

Sandia National Laboratories: *Gamma Irradiation Facility*, 23

Southwest Research Institute: 15, 40

Texas A&M University (TAMU): 14, 15, 28, 33, 39, 72

Texas A&M University: Accelerator Laboratory, 23, 39, 40, 41

University of California, Berkeley (UCB): 14

University of California, Berkeley: *Nuclear Materials Laboratory*, 23, 40 University of Central Florida: 26

University of Chicago: 35

University of Florida (UF): 14, 15, 28, 29, 38, 57

University of Florida (UF): Nuclear Fuels and Materials Characterization, 23, 29

University of Illinois, Urbana-Champaign: 15, 40, 66, 69

University of Michigan (UM): 1, 2, 14, 15, 36, 38, 58, 61

University of Michigan: *Michigan Ion Beam Laboratory* (MIBL), 1, 2, 23, 39, 41, 61

University of Michigan: Irradiated Materials Testing Laboratory, 23

University of Michigan: Michigan Center for Materials Characterization, 23, 40

University of North Texas: 15, 40

University of Oxford: 15, 40

University of Tennessee, Knoxville: 40, 62, 65 University of Wisconsin, Madison: 14

University of Wisconsin: 15, 38, 40, 83

University of Wisconsin: *Ion Beam Laboratory*, 23, 38, 40

University of Wisconsin: Characterization Laboratory for Irradiated Materials, 23

Westinghouse: 14, 33, 80

Westinghouse: *Churchill Laboratory Services*, 23, 40

**Collaborators** 

Baral, Aniruddha University of Illinois, Urbana-Champaign 69

Bruno, Gabriella University of Michigan 61

Chen, Aiping
Los Alamos National Laboratory
57

Chen, Wei-Ying Argonne National Laboratory 55, 57

Chen, Wei-Ying University of Tennessee, Knoxville 65, 76, 78, 79

Chen, Yiren *Argonne National Laboratory* 79

Argonne National Educatory 7

Couet, Adrien University of Wisconsin 83

Field, Kevin University of Michigan 61, 68

He, Lingfeng *Idaho National Laboratory* 74, 75, 83

Hoelzer, David University of Tennessee, Knoxville 65 Hurley, David *Idaho National Laboratory* 74,

75

Jiao, George University of Michigan 61

Le Pape, Yann Oak Ridge National Laboratory 68, 69

Li, Memei Argonne National Laboratory 57

Maloy, Stuart
Los Alamos National Laboratory
71

Muntaha, Ali University of Florida 57

Natesan, Krishnamurti Argonne National Laboratory 79

Pauly, Valentin University of Michigan 61

Saleh, Tarik
Los Alamos National Laboratory
71

Tajuelo Rodriquez, Elena Oak Ridge National Laboratory 68, 69

Taller, Stephen *University of Michigan* 41, 60, 61

Tan, Lizhen
University of Tennessee,
Knoxville 65

Tonks, Michael *University of Florida* 54, 55, 57

White, Joshua Los Alamos National Laboratory 71

Yu, Zefeng Penn State University 57

Yu, Zefeng University of Wisconsin 83

Zinkle, Steven University of Tennessee, Knoxville 65





